

Development of an Integrated Environment for Upper Limb Motion Analysis Studies

by

John M. Giles

A Thesis

Submitted to the Faculty of Graduate Studies

in Partial Fulfillment of the Requirements for the Degree of

Master of Science

In

Electrical Engineering

The University of Manitoba
Department of Electrical Engineering
Winnipeg, Manitoba

April, 1994



National Library
of Canada

Acquisitions and
Bibliographic Services Branch

395 Wellington Street
Ottawa, Ontario
K1A 0N4

Bibliothèque nationale
du Canada

Direction des acquisitions et
des services bibliographiques

395, rue Wellington
Ottawa (Ontario)
K1A 0N4

Your file *Votre référence*

Our file *Notre référence*

The author has granted an irrevocable non-exclusive licence allowing the National Library of Canada to reproduce, loan, distribute or sell copies of his/her thesis by any means and in any form or format, making this thesis available to interested persons.

L'auteur a accordé une licence irrévocable et non exclusive permettant à la Bibliothèque nationale du Canada de reproduire, prêter, distribuer ou vendre des copies de sa thèse de quelque manière et sous quelque forme que ce soit pour mettre des exemplaires de cette thèse à la disposition des personnes intéressées.

The author retains ownership of the copyright in his/her thesis. Neither the thesis nor substantial extracts from it may be printed or otherwise reproduced without his/her permission.

L'auteur conserve la propriété du droit d'auteur qui protège sa thèse. Ni la thèse ni des extraits substantiels de celle-ci ne doivent être imprimés ou autrement reproduits sans son autorisation.

ISBN 0-315-92256-7

Canada

Name _____

Dissertation Abstracts International is arranged by broad, general subject categories. Please select the one subject which most nearly describes the content of your dissertation. Enter the corresponding four-digit code in the spaces provided.

Applied

Sciences

SUBJECT TERM

0541

U·M·I

SUBJECT CODE

Subject Categories

THE HUMANITIES AND SOCIAL SCIENCES

COMMUNICATIONS AND THE ARTS

Architecture 0729
 Art History 0377
 Cinema 0900
 Dance 0378
 Fine Arts 0357
 Information Science 0723
 Journalism 0391
 Library Science 0399
 Mass Communications 0708
 Music 0413
 Speech Communication 0459
 Theater 0465

EDUCATION

General 0515
 Administration 0514
 Adult and Continuing 0516
 Agricultural 0517
 Art 0273
 Bilingual and Multicultural 0282
 Business 0688
 Community College 0275
 Curriculum and Instruction 0727
 Early Childhood 0518
 Elementary 0524
 Finance 0277
 Guidance and Counseling 0519
 Health 0680
 Higher 0745
 History of 0520
 Home Economics 0278
 Industrial 0521
 Language and Literature 0279
 Mathematics 0280
 Music 0522
 Philosophy of 0998
 Physical 0523

Psychology 0525
 Reading 0535
 Religious 0527
 Sciences 0714
 Secondary 0533
 Social Sciences 0534
 Sociology of 0340
 Special 0529
 Teacher Training 0530
 Technology 0710
 Tests and Measurements 0288
 Vocational 0747

LANGUAGE, LITERATURE AND LINGUISTICS

Language
 General 0679
 Ancient 0289
 Linguistics 0290
 Modern 0291
 Literature
 General 0401
 Classical 0294
 Comparative 0295
 Medieval 0297
 Modern 0298
 African 0316
 American 0591
 Asian 0305
 Canadian (English) 0352
 Canadian (French) 0355
 English 0593
 Germanic 0311
 Latin American 0312
 Middle Eastern 0315
 Romance 0313
 Slavic and East European 0314

PHILOSOPHY, RELIGION AND THEOLOGY

Philosophy 0422
 Religion
 General 0318
 Biblical Studies 0321
 Clergy 0319
 History of 0320
 Philosophy of 0322
 Theology 0469

SOCIAL SCIENCES

American Studies 0323
 Anthropology
 Archaeology 0324
 Cultural 0326
 Physical 0327
 Business Administration
 General 0310
 Accounting 0272
 Banking 0770
 Management 0454
 Marketing 0338
 Canadian Studies 0385
 Economics
 General 0501
 Agricultural 0503
 Commerce-Business 0505
 Finance 0508
 History 0509
 Labor 0510
 Theory 0511
 Folklore 0358
 Geography 0366
 Gerontology 0351
 History
 General 0578

Ancient 0579
 Medieval 0581
 Modern 0582
 Black 0328
 African 0331
 Asia, Australia and Oceania 0332
 Canadian 0334
 European 0335
 Latin American 0336
 Middle Eastern 0333
 United States 0337
 History of Science 0585
 Law 0398
 Political Science
 General 0615
 International Law and Relations 0616
 Public Administration 0617
 Recreation 0814
 Social Work 0452
 Sociology
 General 0626
 Criminology and Penology 0627
 Demography 0938
 Ethnic and Racial Studies 0631
 Individual and Family Studies 0628
 Industrial and Labor Relations 0629
 Public and Social Welfare 0630
 Social Structure and Development 0700
 Theory and Methods 0344
 Transportation 0709
 Urban and Regional Planning 0999
 Women's Studies 0453

THE SCIENCES AND ENGINEERING

BIOLOGICAL SCIENCES

Agriculture
 General 0473
 Agronomy 0285
 Animal Culture and Nutrition 0475
 Animal Pathology 0476
 Food Science and Technology 0359
 Forestry and Wildlife 0478
 Plant Culture 0479
 Plant Pathology 0480
 Plant Physiology 0817
 Range Management 0777
 Wood Technology 0746
 Biology
 General 0306
 Anatomy 0287
 Biostatistics 0308
 Botany 0309
 Cell 0379
 Ecology 0329
 Entomology 0353
 Genetics 0369
 Limnology 0793
 Microbiology 0410
 Molecular 0307
 Neuroscience 0317
 Oceanography 0416
 Physiology 0433
 Radiation 0821
 Veterinary Science 0778
 Zoology 0472
 Biophysics
 General 0786
 Medical 0760

Geodesy 0370
 Geology 0372
 Geophysics 0373
 Hydrology 0388
 Mineralogy 0411
 Paleobotany 0345
 Paleocology 0426
 Paleontology 0418
 Paleozoology 0985
 Palynology 0427
 Physical Geography 0368
 Physical Oceanography 0415

HEALTH AND ENVIRONMENTAL SCIENCES

Environmental Sciences 0768
 Health Sciences
 General 0566
 Audiology 0300
 Chemotherapy 0992
 Dentistry 0567
 Education 0350
 Hospital Management 0769
 Human Development 0758
 Immunology 0982
 Medicine and Surgery 0564
 Mental Health 0347
 Nursing 0569
 Nutrition 0570
 Obstetrics and Gynecology 0380
 Occupational Health and Therapy 0354
 Ophthalmology 0381
 Pathology 0571
 Pharmacology 0419
 Pharmacy 0572
 Physical Therapy 0382
 Public Health 0573
 Radiology 0574
 Recreation 0575

Speech Pathology 0460
 Toxicology 0383
 Home Economics 0386

PHYSICAL SCIENCES

Pure Sciences

Chemistry
 General 0485
 Agricultural 0749
 Analytical 0486
 Biochemistry 0487
 Inorganic 0488
 Nuclear 0738
 Organic 0490
 Pharmaceutical 0491
 Physical 0494
 Polymer 0495
 Radiation 0754
 Mathematics 0405
 Physics
 General 0605
 Acoustics 0986
 Astronomy and Astrophysics 0606
 Atmospheric Science 0608
 Atomic 0748
 Electronics and Electricity 0607
 Elementary Particles and High Energy 0798
 Fluid and Plasma 0759
 Molecular 0609
 Nuclear 0610
 Optics 0752
 Radiation 0756
 Solid State 0611
 Statistics 0463

Applied Sciences

Applied Mechanics 0346
 Computer Science 0984

Engineering
 General 0537
 Aerospace 0538
 Agricultural 0539
 Automotive 0540
 Biomedical 0541
 Chemical 0542
 Civil 0543
 Electronics and Electrical 0544
 Heat and Thermodynamics 0348
 Hydraulic 0545
 Industrial 0546
 Marine 0547
 Materials Science 0794
 Mechanical 0548
 Metallurgy 0743
 Mining 0551
 Nuclear 0552
 Packaging 0549
 Petroleum 0765
 Sanitary and Municipal 0554
 System Science 0790
 Geotechnology 0428
 Operations Research 0796
 Plastics Technology 0795
 Textile Technology 0994

PSYCHOLOGY

General 0621
 Behavioral 0384
 Clinical 0622
 Developmental 0620
 Experimental 0623
 Industrial 0624
 Personality 0625
 Physiological 0989
 Psychobiology 0349
 Psychometrics 0632
 Social 0451



DEVELOPMENT OF AN INTEGRATED ENVIRONMENT FOR UPPER
LIMB MOTION ANALYSIS STUDIES

BY

JOHN M. GILES

A Thesis submitted to the Faculty of Graduate Studies of the University of Manitoba in partial fulfillment of the requirements for the degree of

MASTER OF SCIENCE

© 1994

Permission has been granted to the LIBRARY OF THE UNIVERSITY OF MANITOBA to lend or sell copies of this thesis, to the NATIONAL LIBRARY OF CANADA to microfilm this thesis and to lend or sell copies of the film, and UNIVERSITY MICROFILMS to publish an abstract of this thesis.

The author reserves other publications rights, and neither the thesis nor extensive extracts from it may be printed or otherwise reproduced without the author's permission.

ABSTRACT

The purpose of this work was to develop further the University of Manitoba Motion Analysis System (UM²AS) to analyze upper limb (UL) motion which will aid people with dysfunction of the UL. Several development phases of UM²AS have already been completed by R. Safae-Rad, and K. Macleod. The current phase accomplished three objectives: 1) reduce the frequency of an UL motion marker disappearing from the view of two cameras, 2) enhance the software to make the system more suitable for the clinical environment, and 3) explore the effect of error in the input data propagating through UM²AS. The reduction of UL motion marker loss is accomplished by using three cameras in an orthogonal configuration. This gives UM²AS the ability to view more of the experimental area during the experiment and thus increases the chance of viewing the markers. The software was first enhanced by writing it in the language C which has support for a graphical user interface (GUI) type of program. The program was then developed into a largely mouse driven, pop-up window GUI. A system such as this was found to be easy to use and required minimal computer skills. Error in the system was found to be largely due to lens distortion of the image and the marker being either partially hidden or engulfed in surrounding noise in the image. This causes the camera view coordinates of UM²AS to be perturbed. The maximum perturbation due to lens distortion was found to be 0.5 pixel widths and for diminished visibility the perturbation increased to 12.5 pixel widths. Because there is error in the camera view coordinates it is crucial to discover how sensitive UM²AS is to this error. Error propagation or sensitivity was explored by perturbing the input parameters for calculating the calibration parameters and for calculating the three-dimensional real world coordinates of the markers. The sensitivity analysis revealed that the small error in the calibration parameters has a tolerable effect on the calculated real world coordinates. The largest contribution to the error in the calculated real world coordinates is caused by the error in the camera view coordinates of the UL.

ACKNOWLEDGMENTS

I would like to thank Professors Ed Shwedyk and Juliette Cooper for their guidance and comments that helped me develop UM²AS into what it is today. A special thanks to Gord Toole "THE TOOLE MAN" for his technical support and in providing the needed materials to make this thesis a reality.

I would also like to thank W.H. Lehn and D.J. Thomson for permitting me to draw on their knowledge respectively in image processing and optoelectronics. Their help contributed to the completion of this thesis.

For financial support I would like to thank the Rehabilitation Centre for Children Research Foundation.

TABLE OF CONTENTS

Abstract	i
Acknowledgments	ii
Table of Contents	iii
List of Tables	v
List of Figures	vi
Definitions	viii
1. Introduction	1
2. Upper Limb Model, Marker Placement, and Equipment used in UM ² AS	6
2.1 Model of the Upper Limb	7
2.2 Apparatus Placed on the Subject	9
2.3 Equipment Used by UM ² AS	11
2.3.1 Commercially Available Equipment Used	12
2.3.2 Video Information Flow Through Equipment	16
2.3.3 Calibration Box	17
2.4 Calculating the Upper Limb Real World Marker Coordinates	19
3 Software Design and Development	24
3.1 The Overall Program	24
3.2 Design Criteria	26
3.3 Main Menu For Integrated Environment	27
3.4 Calculating Camera Calibration Parameters	28
3.5 Marker Coordinate Digitization	35
3.6 Real World (X, Y, Z) Coordinate Calculation	41

3.7	Calculate Euler Angles	44
4.	Error Identification and its Progression Through UM ² AS	46
4.1	Determining the Aspect Ratio of the Cameras	47
4.2	Determining the Magnitude of Error in the Camera View Centroids	52
4.3	Sensitivity Analysis	53
4.3.1	Calibration Parameter (CP) Sensitivity	56
4.3.2	Proposed Real World Coordinate Sensitivity Method	58
5	Conclusions	61
6	References	64
7	Appendices	
A	Derivation of Euler Angle Formulas (Angular Rotations)	67
B	Derivation of Calibration Parameter and Real World Coordinate Calculation Formulas	76

LIST OF TABLES

2.1	Normal Motion for the Shoulder, Elbow, and Wrist Joint Regions	9
2.2	Equipment Used in the Motion Analysis System	11
4.1	Results of Relative Distance Error Test	52
4.2	Relative Error of each L Parameter	58

LIST OF FIGURES

2.1	Order of Euler Angle Rotations	8
2.2	Marker Placement for an 8 DOF UL Model	10
2.3	Overhead View of Laboratory	12
2.4	Side View of Camera and Lighting Equipment	13
2.5	Three Camera Orientation with Respect to the Viewing Space	14
2.6	Representative Picture of Equipment in the Lab	15
2.7	Video Information Flow Diagram	16
2.8	Calibration Box and Control Ball Attachment	18
2.9	Criterion for Choosing between Three Calculated Points	22
3.1	Block Diagram of Complete Program	25
3.2	Flow Structure of the Program	26
3.3	Main Menu of the Program	27
3.4	Calibration Parameter Calculation Menu	28
3.5	Contents of *.msr and *.cp1	29
3.6	Calibration Parameters Start Up Information Option	30
3.7	Calibration and Measured Data File Name Selection	31
3.8	Threshold Function and Dialog Box	32
3.9	Reference Marker Acquisition Menu	32
3.10	Manual Digitization Flow Chart	34
3.11	Motion Data Acquisition Main Menu	35
3.12	Format of a camera 1 Data File (*.da1)	36
3.13	Start Up Information for Motion Data Acquisition	37
3.14	Automatic Digitization Flow Chart	38
3.15	Verify Digitization Flow Chart	40
3.16	Menu for X, Y, and Z Coordinate Calculation	41
3.17	File Format for a Typical *.tdc	42

3.18	Start Up Information	42
3.19	Menu for Calibration and Marker Motion Data Files	43
3.20	Main Euler Angle Calculation Menu	44
3.21	Euler Angle Data File Format (*.wst)	45
4.1	Rotating Apparatus for Checking Distortion	48
4.2	Distance Between Selected Marker Pairs	49
4.3	Corrected Distances Between Selected Marker Pairs	51
4.4	Polar Coordinate Representation of Perturbation	55
4.5	Flow Chart of Error Flow from the Control Ball Camera View Coordinates to the Calibration Parameters	57
4.6	Flow Chart of Error Propagation from the Marker Camera View Coordinates to the Calculated Real World Coordinates	59
A.1	Stick Diagram and Vector Directions for the Upper Limb Model	71

DEFINITIONS

UM ² AS	-	University of Manitoba Motion Analysis System
UL	-	upper limb
DOF	-	degrees of freedom
VCR	-	video cassette recorder
CP	-	calibration parameter
CB	-	control ball
LED	-	light emitting diode
CCD	-	charged-coupled device
SVGA	-	super video graphics adapter
PC	-	personal computer
RGB	-	red, green, and blue
Pixel	-	a computer monitor unit of area. Its sides are defined as one unit by one unit which is termed a pixel width in this thesis
2-D Centroid	-	the centre of an object found in a two dimensional digitized image
3-D Centroid	-	the centre of an object located in a three dimensional space
(U_i^k, V_i^k)	-	2-D centroid for upper limb or control ball marker i in camera view k
$(X_i^{CB}, Y_i^{CB}, Z_i^{CB})$	-	3-D tape measured centroid for control ball i
$(X_i^{mn}, Y_i^{mn}, Z_i^{mn})$	-	calculated 3-D centroid for upper limb marker i in relation to camera m and n
(L_1^k, \dots, L_{11}^k)	-	calibration parameters from one to eleven for camera k

CHAPTER I

INTRODUCTION

The upper limb (UL) is very important because with it all essential daily activities such as feeding, dressing, and/or personal care are performed (DOF) [4]. The UL is comprised of many joints and muscles that work together to perform these essential daily activities and is a very redundant device with approximately 87 degrees of freedom [4,12]. Dysfunction of UL joints and/or muscles resulting from injury and/or disease may reduce the range of motion available which may make essential daily activities difficult if not impossible to perform [4]. Before any conclusions about abnormal motion can be made a normal motion baseline must be obtained experimentally using subjects with a normal range of motion. Therefore studies of the normal range of UL motion during performance of selected essential activities must be carried out. The results of these studies may be used to develop strategies for adaptation to and compensation for motion dysfunction and also could be used to aid in designing an UL prosthesis whose function is similar to that of an actual limb.

Performing selected daily activities such as combing hair, personal hygiene, eating with utensils, and drinking from a cup require the UL to move in three-dimensional space. Therefore, the main criterion for any method of acquiring UL motion data for the purpose of analyzing functional motion is that it must have the capability of collecting three-dimensional information about the UL. The most common methods of acquiring motion data are: a) goniometry [15], b) cinematography [15], c) optoelectronic techniques [3], and d) television video techniques [15].

Goniometry is the measurement of the angle formed by the joint between two limb segments. An electrogoniometer is an electronic device that is attached to limb segments that measures the rotation at the joint. The advantages of the electrogoniometer method are that it is inexpensive and the output signal is available immediately for recording or conversion

into a computer data file [15]. The disadvantages are that it may require an excessive length of time to fit and align, movement can be encumbered by straps and cables, and complex multiaxial electrogoniometers are required for joints which do not move as hinge joints [15].

Cinematography involves placing reflective markers on UL segments and filming the UL motion using two or more 8mm or 16mm cinefilm cameras [15]. The advantages of using this method are minimal encumbrance and the data format is in terms of absolute marker coordinates [15]. The main disadvantage is the high cost of the needed film and equipment to extract three dimensional coordinate data [15].

Optoelectronic systems (eg. Selspot) use LEDs as markers to define the UL segment being studied and a lens in front of a Lateral-photo-effect diode as a camera (two or more of these cameras are used) [3]. The advantages of this method are all the major equipment used is available commercially, and encumbrance to UL motion is minimal [3]. The disadvantages for a clinical environment are: a) wires will run on the UL to power all the LEDs, b) the diodes used are infrared therefore they capture the all infrared sources such as sunlight and radiant heat from radiators or heat ducts, and c) infrared cannot be seen by the human eye and therefore the information is not obtainable until the experiment is completed. Because the markers are infrared, no possible intervention during the course of the experiment could be performed because the operator does not know if there was an error until the experiment is completed.

For three dimensional motion analysis the television video recording technique method requires that the motion be viewed by at least two or more CCD cameras and anatomical landmarks of interest be defined using reflective markers [15]. The images viewed by the cameras are recorded on video tapes. The images from the video tapes can then be processed with an image processing board and an IBM PC compatible computer to extract the three dimensional location of the markers. Video based systems are accurate, relatively inexpensive, and provide a reasonably fast turnaround for data collection [11].

They also provide a permanent visual record which is of particular importance, especially in a clinical setting [11]. The disadvantage to video based systems is that the recorded camera views have light noise that can be mistaken for markers or a marker can be engulfed by the noise.

Commercial video based systems are relatively expensive, therefore the development of the University of Manitoba Motion Analysis System (UM²AS) was started. The development of UM²AS started in 1985 with the work of Safaee-Rad [12]. At this stage efforts were focussed on obtaining the basis for a system that could acquire needed UL motion data. The earliest version of UM²AS had software written in FORTRAN, used two CCD cameras, and the data collection process per VCR frame was completely automatic. UM²AS allowed for no intervention to correct any errors in the frame data as they occurred. Motion was captured and stored on two video tapes at the VCR sampling rate of 30 frames per second. A flash lamp was used to synchronize the two video tapes. Reflective white markers were placed on the UL to define the segments being studied. The centre coordinates of the round white markers were found for each of the two-dimensional camera views. These were termed camera view coordinates (CVCs) which were subsequently used to calculate the three-dimensional real world coordinates of the markers for a given frame. The three-dimensional real world coordinates were then used to calculate the angular motion of the joints in the UL. Unfortunately, being completely automatic, the system allowed for no intervention by the operator to correct or even know if any processing errors had occurred.

The second phase of UM²AS development made extracting the UL motion data completely manual. "In this method, the marker locations within each digitized image must be segmented manually by surrounding each marker with a rectangle" [10,p. 2]. This method of marker detection, while achieving a high degree of accuracy, was a very time consuming process because a large amount of operator intervention was required, thereby slowing the motion data collection process [10].

The third phase of development made the detection of markers more automatic and simplified the method of obtaining marker locations [10]. Manual detection of a marker only involved placing a cursor over the image of the marker on a television screen. The software, now written in C, then calculated the centroid of the marker automatically. The first two frames of video information were digitized manually to find the centre of the markers in the camera view. Then the position of the markers in the subsequent frames was approximated by linear extrapolation of the location of the marker centroid in the previous two frames. This made the data collection process more automatic thereby removing more of the repetitive tasks from the operator and delegating them to the computer. The program also allowed the option of verifying that the correct camera view coordinate (U,V) of the marker was given. This made it possible to correct any processing errors.

After this version was used in a study of functional UL motion, it was found that three aspects of UM²AS required further refinement and research:

A method of dealing with missing markers was needed. The addition of a third camera to UM²AS was proposed as a way to decrease the loss of UL marker motion data. Two independent camera views of the same marker are needed to calculate the three dimensional coordinate of the marker. Occasionally a marker will be hidden from the view of the camera or engulfed in noise. The addition of the third camera adds some redundancy to UM²AS and an additional camera view that can possibly make up for one camera not seeing a marker.

The software of UM²AS needed to be more operator friendly. Before the current work was undertaken the software for UM²AS was written in C and FORTRAN and was not very operator friendly. In addition the existing UM²AS did not allow the operator to make changes to correct errors that were made previously. Further software development was therefore needed to make the system more suitable for the commercial market.

Sources of input data error had to be identified and isolated; the effect of input data propagating through UM²AS must be quantified and then eliminated with the appropriate

measures.

Chapter II documents the eight DOF mathematical model of the UL used, the linear algebra used to calculate the three dimensional coordinates of the UL markers from the three sets of camera view coordinates, and lists the equipment used in UM²AS. Chapter III presents the software enhancements. Chapter IV explores potential sources of input data error and then presents a method of measuring how this error propagates through UM²AS. Lastly, Chapter V contains conclusions and recommendations for further development of UM²AS.

CHAPTER II

Upper Limb Model, Marker Placement and Equipment used in UM²AS

To create an upper limb (UL) motion analysis system such as the University of Manitoba Motion Analysis System (UM²AS) requires essentially three steps. A model of the UL must be conceptualized, a method of highlighting the limb segments needs to be developed, and finally a method of calculating the three-dimensional (3-D) marker centroids of the UL segments must be created. In order to study the motion of the UL a mathematical model is required in order to analyze 3-D motion of the human UL. The model used in UM²AS is that described and developed by Safae-Rad in which the UL is considered to be a four joint anatomical device with a total of eight degrees of freedom (DOF) [12]. Based on experiments performed by Safae-Rad this model is considered to be adequate for the study of functional UL motion [12].

To use the UL model a means of highlighting or defining the segments of the UL is required. There are a number of ways of doing this such as using LEDs [3] and light reflective markers attached to anatomical landmarks [12]. The method used in UM²AS is that of ping pong balls covered with 3M reflective tape and placed at defined locations on the UL in order to describe the eight DOF model properly. The information that the model provides is extracted by UM²AS, using the television video method to acquire the 3-D marker centroids. This method consists of simultaneously storing images of the UL motion, viewed by two or more cameras, on two or more video tapes. The two-dimensional (2-D) camera view UL marker centroids can then be extracted from these tapes and stored in computer data files.

The 3-D UL reflective marker centroids can be derived from the camera view data. This is done by calibrating UM²AS, i.e. by relating the 2-D control ball (CB) marker centroids to the known 3-D measured CB centroids by using 11 calibration parameters (CPs). The 2-D centroids of the UL motion along with the CPs are then used to obtain the

calculated 3-D centroids of the UL markers. UM²AS uses equipment that is available commercially, therefore the system is easy to create and relatively inexpensive.

2.1 Model of the Upper Limb

All major joints of the body have six degrees of freedom: three translations and three rotations [15]. Typically, translation is small and ignored in motion studies; therefore in UL studies done to date only rotational motion of the UL was considered. The orientation of a segment of the UL is defined by its position relative to three orthogonal planes (sagittal, frontal, and transverse) or by its angular motion about three orthogonal axes [15].

The three rotational motions $(\phi_i, \theta_i, \psi_i)$ are defined with respect to three orthogonal axes using the Euler angle method (shown in detail in Appendix A). Several Euler angle systems have been used for this type of motion analysis with the difference being the order in which the angles are applied. The order of rotation about the specified axes is important in order to describe the joint motion uniquely. The order chosen here is that used by Safaee-Rad [12].

The auxiliary axis system is initially oriented at the position (x_i^T, y_i^T, z_i^T) which is shown in Figure 2.1a. The rotation order is shown in Figure 2.1 where ϕ_i is the first rotation about the z_i^T axis. It rotates the auxiliary axis system into a new orientation called (x_i^1, y_i^1, z_i^1) . Next, is the rotation about the x_i^1 axis, θ_i , which rotates the axis system to the orientation labelled (x_i^2, y_i^2, z_i^2) . Lastly, ψ_i is the rotation about the y_i^2 axis which puts the axis system in its final auxiliary orientation (x_i, y_i, z_i) as shown in Figure 2.2c.

Studies done in the past represent the shoulder joint as being three DOF [5], the wrist joint also with three DOF [16], and the elbow joint with two DOF [5]. The elbow is modelled as a two DOF spherical joint which therefore has two rotations [5]. The elbow joint model includes the angular rotation. In the studies done with UM²AS to date (eating with a fork or spoon, drinking from a cup) the shoulder, elbow, and wrist joint were also

modelled respectively with three, two, and three DOF.

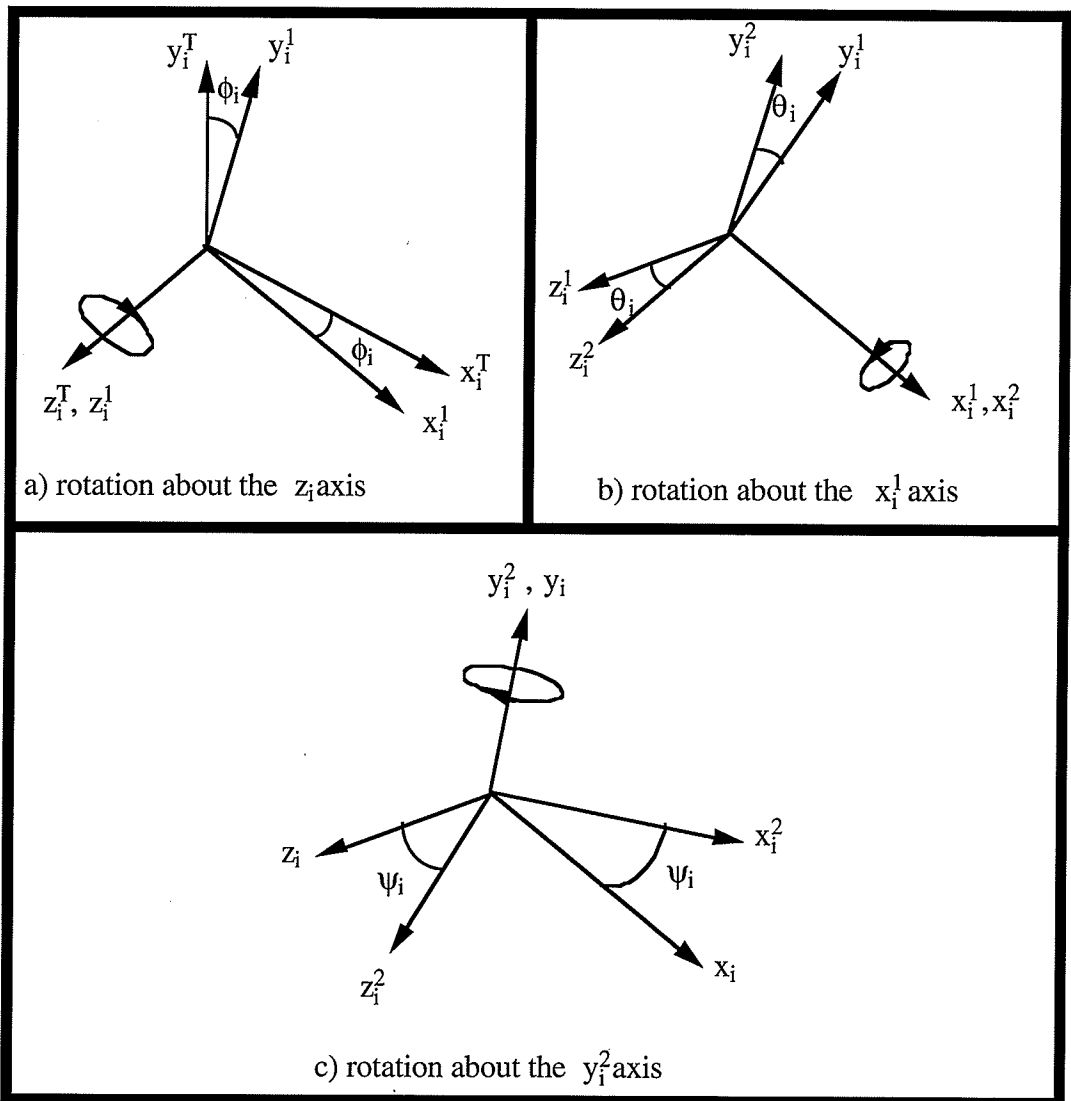


Figure 2.1 Order of Euler Angle Rotations [7]

of radius rotating about the ulna at the radioulnar joints. The superior radio-ulnar joint is not actually at the elbow but can be effectively referenced to the elbow. The equations for angular rotation in the shoulder, wrist and elbow region are given in Appendix A. The normal range of the angular rotations for the shoulder joint, elbow region joints, and wrist joint is given in Table 2.1 [1,6,8].

Table 2.1

Joint	Angular Rotations	Anatomical Terms	Range of Normal Motion in degrees
Shoulder	ϕ_1	Flexion Extension	0 - 180 0 - 60
	θ_1	Abduction Adduction	0 - 180 0 - 75
	ψ_1	Internal Rotation External Rotation	0 - 90 0 - 90
Elbow	ϕ_2	Flexion Extension	0 - 150 0 - 10
	ψ_2	Pronation Supination	0 - 90 0 - 90
Wrist	ϕ_3	Flexion Extension	0 - 80 0 - 70
	θ_3	Radial Deviation Ulnar Deviation	0 - 20 0 - 30
	ψ_3	Internal Rotation External Rotation	approx. zero approx. zero

Normal Motion for the Shoulder, Elbow, and Wrist Joint Region

2.2 Apparatus Placed on the Subject

The UL is modelled as having only eight DOF or in other words, eight angular rotations [11]. To obtain all eight rotations, seven markers must be attached to the subject's UL as in Figure 2.2. Markers 1 and 2 are placed on the superior surface of the acromion process of the scapula [2]. Marker 3 is placed on the superior aspect of the arm segment, 3 cm distal to the lateral border of the acromion process [2]. Marker 4 is placed on the lateral epicondyle of the humerus [2]. Markers 5 and 6 are mounted on a rod which is attached to the distal aspect of the dorsum of the ulna and the radius in line with their respective styloid processes [2]. Marker 7 is placed over the dorsal aspect of the head of the third metacarpal

[2].

An experiment was conducted to determine the "optimum" size and reflectiveness of the anatomical markers. Ping-pong balls (diameter = 34 mm), styrofoam balls (diameter = 19 and 34 mm) and solid plastic balls (diameter = 13 mm) were used to test for size. Green and white reflective tapes respectively were used to determine the best reflectiveness. Ping-pong balls covered with white reflective tape proved to be the best combination for

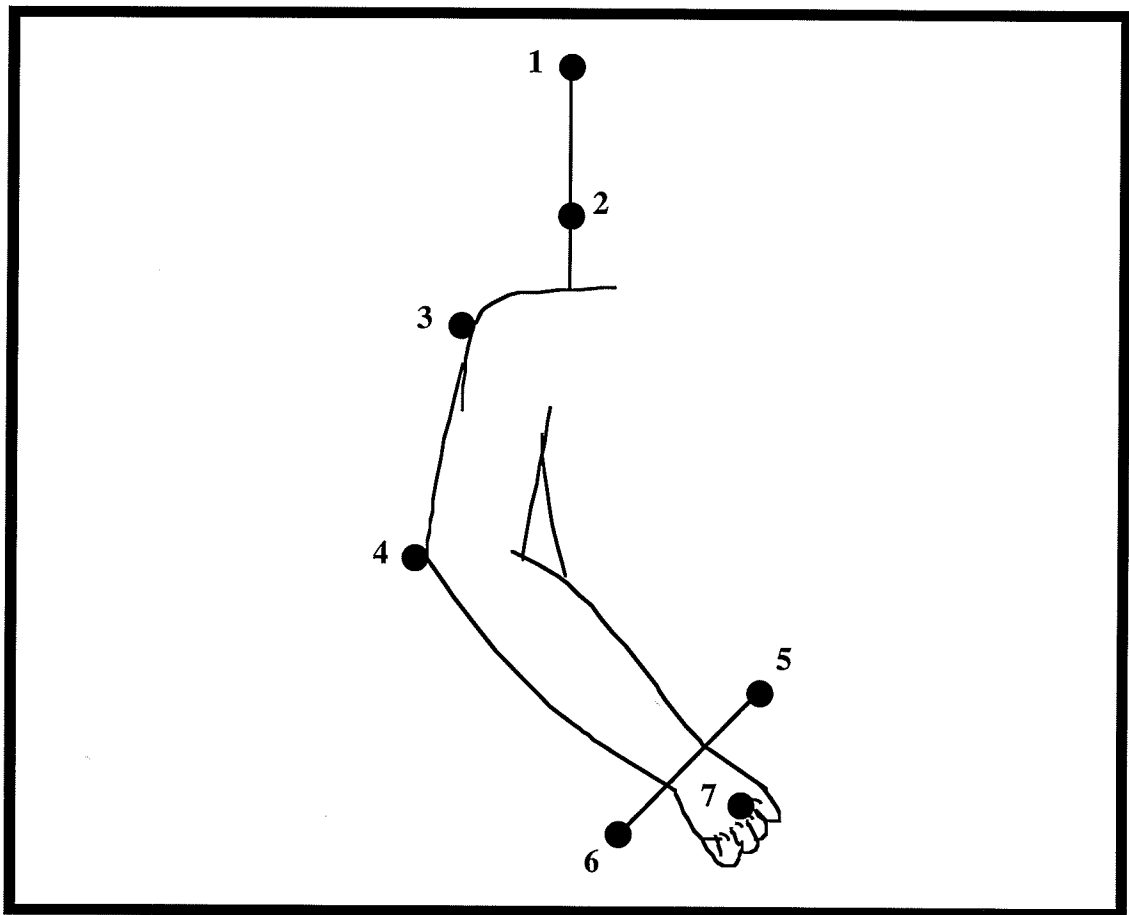


Figure 2.2 Marker Placement for an 8 DOF UL Model

processing the image. The size of the marker and the reflectiveness of the tape decreased the frequency of the marker becoming engulfed in background noise therefore making it easier to calculate its camera view coordinate (version 2 of UM²AS used solid plastic balls). The subject also wears a dark, long-sleeved turtleneck shirt in order to ensure a

highly contrasting background for the white reflective markers. This reduces the noise produced by oils in the skin that reflect white light at the same intensity as the UL markers.

2.3) Equipment Used in UM²AS

This section describes the function of the commercial and specially manufactured equipment used in UM²AS. Table 2.2 lists the equipment needed for UM²AS.

Table 2.2

Quantity	Item
3	black and white CCD video cameras
3	zoom lenses
2	camera stands
3	video cassette recorders, one with frame-by-frame replay and frame counting capabilities
3	40w 120v light bulbs
3	light shrouds
2	light stands
1	clamp (mounts camera to ceiling)
1	PC computer with PIPEZ image processing and acquisition board
1	monitor with computer and RGB image channels
3	monochrome monitors
1	calibration jig and accessories

Equipment Used in the Motion Analysis System

2.3.1) Commercially Available Equipment Used

The laboratory used to perform the experiments is partitioned into two areas: 1) the studio and 2) the equipment room. The studio occupies an area of 3.6 m x 3.6 m. This provides enough space for the cameras to view a 1 m³ space as shown from an overhead view in figure 2.3. This size of viewing space is needed to allow enough room for the

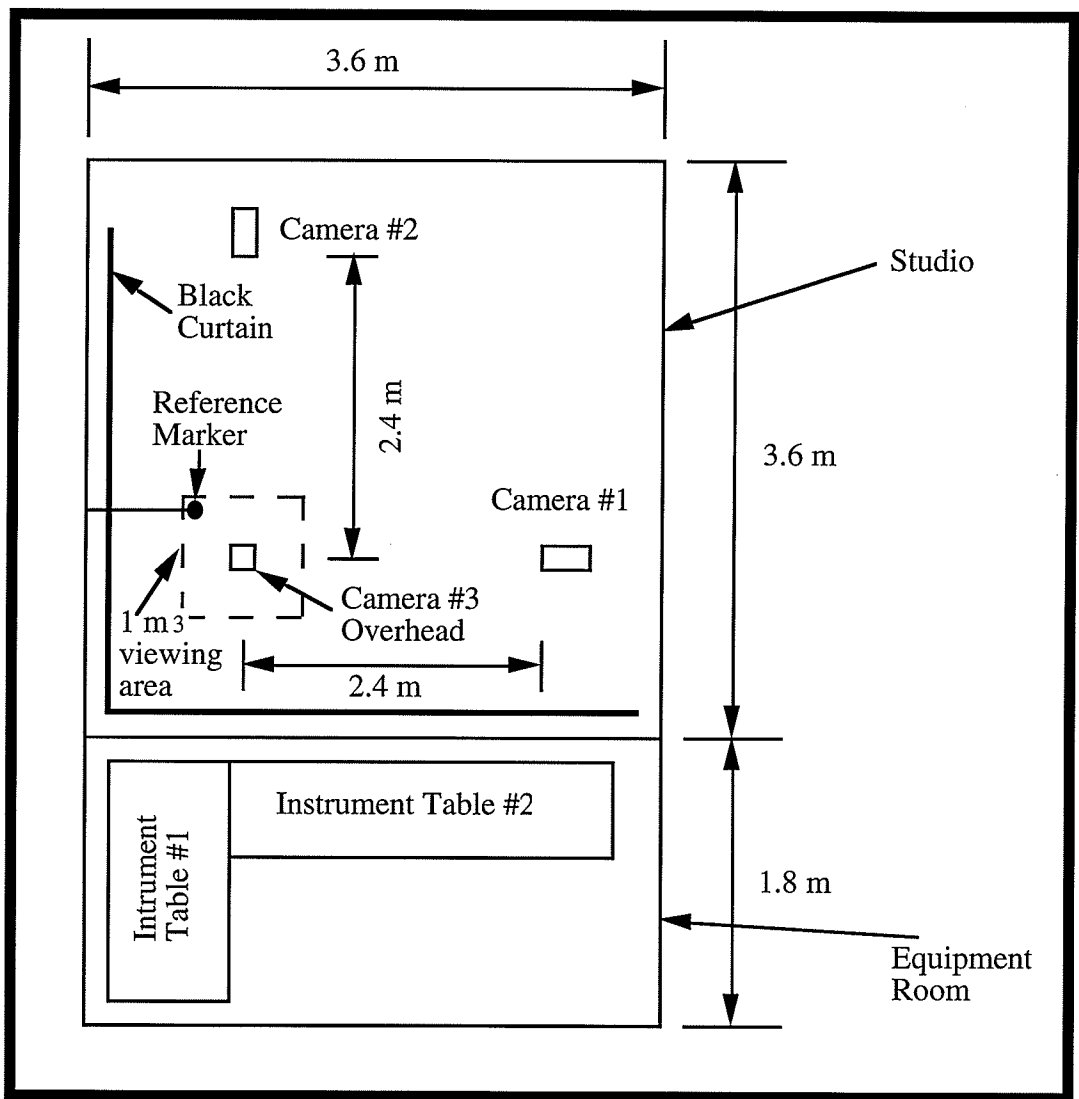


Figure 2.3 Overhead View of Laboratory

subject to perform the UL motion experiments without the limb moving out of the viewing space. Located in the viewing space is a reference marker shown in Figure 2.3. It can be

seen by all three cameras (camera and lighting apparatus is shown in Figure 2.4) as a common reference. The reference marker is used to compensate for any horizontal and/or vertical shifts that may occur when the image is acquired. Covering the wall (shown in Figure 2.3) is a black curtain; this provides a dark background for the recorded images and reduces light noise by providing an effective contrast to the markers.

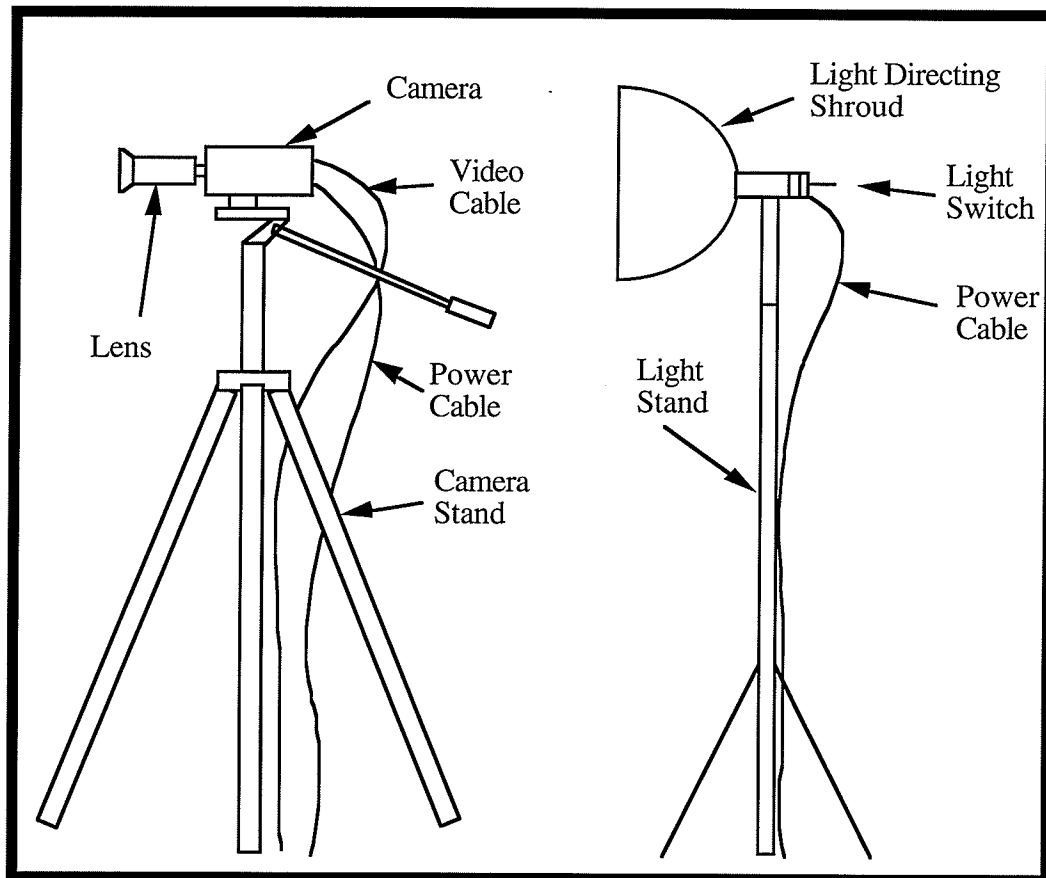


Figure 2.4 Side View of Camera and Lighting

The motion experiments are performed in the studio in front of three CCD cameras. These cameras are placed on adjustable stands and are arranged in the studio so that all three see the same viewing space. The cameras are set along the X, Y, and Z axes of the real world coordinate system (Figure 2.5) and are placed equidistant from the point where their centers of view intersect (2.4 m from intersection point). It is essential that the cameras be at the same distance from the centre of the viewing space, set at the same focal length, and that the centres of their views intersect. This is to minimize the error in the three

dimensional calculated real world coordinates. A lamp with a 40 watt bulb is placed behind each camera to direct light onto the reflective markers in order to enhance visibility (Figure 2.4).

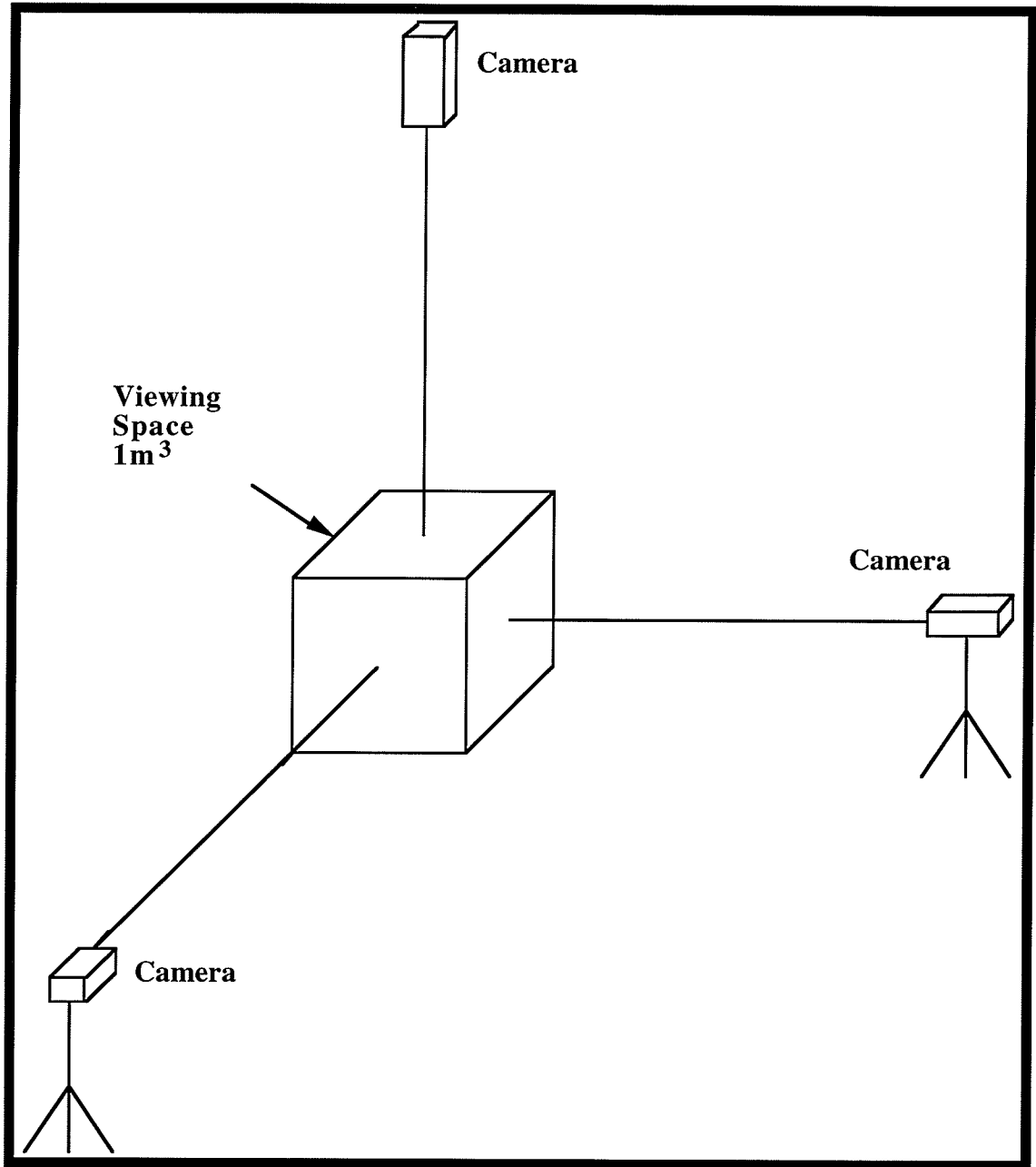


Figure 2.5 Three Camera Orientation with respect to the Viewing Space

The equipment room is also shown in Figure 2.3 and occupies an area of 1.8 m x 3.6 m. Two instrument tables are located here, orientated as in Figure 2.3. Instrument

Table #1 (shown from a front view in Figure 2.6 a) holds three video cassette recorders (VCR's) and three monochrome monitors, one for each VCR. VCR #1 has a frame-by-frame advance feature. The monitors are used to view what is being seen by the three cameras

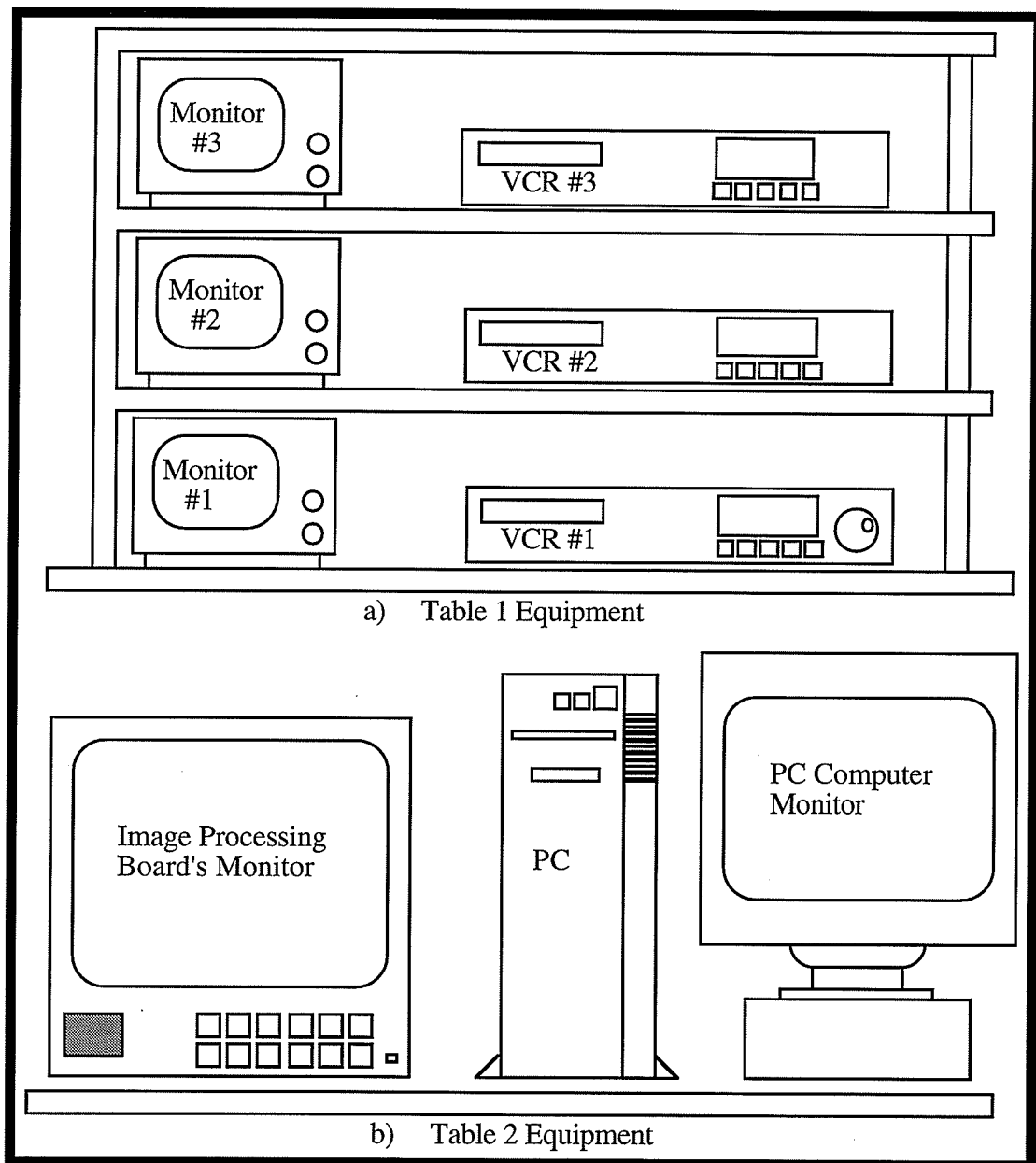


Figure 2.6 Representative Picture of the Equipment in the Lab

and what is being taped on the VCR's. Instrument table #2 (shown in figure 2.6 b), holds a 486 computer, computer monitor, and a monitor for the computer's image processing board. The computer used is a 486 PC with a MATROX PIPEZ image processing board,

and a SVGA graphics card. The image processing board monitor is a Sony monitor with RGB image channels. The equipment is set up on the two tables in this configuration to allow the operator easy access.

2.3.2 Video Information Flow Through Equipment

Video information flow of the system can be broken into two phases. In Phase I the video information is stored on three video tapes. In Phase II the marker centres are extracted from the video tapes and stored in a computer file.

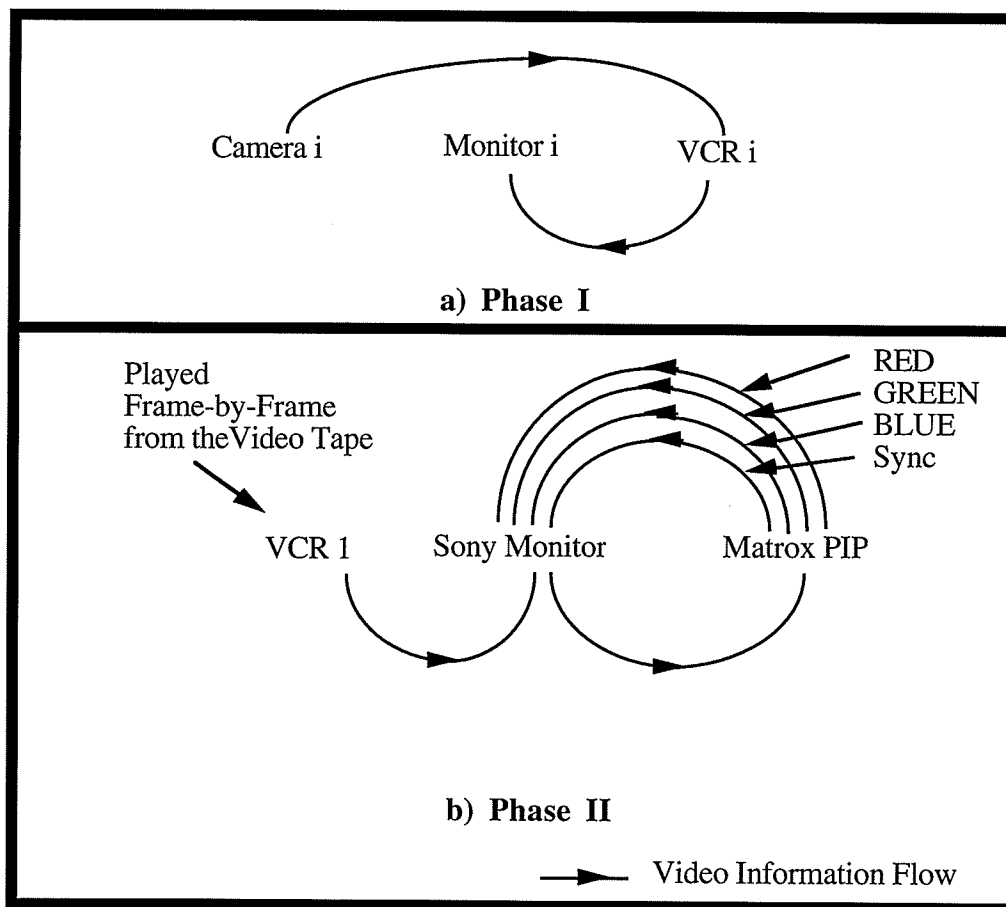


Figure 2.7 Video Information Flow Diagram

In Phase I (Figure 2.7a) an image is captured by a camera and is sent to its VCR which records the image on Beta tape. The image is also sent through the VCR to a monitor

to be viewed by the operator. At the end of Phase I there are three tapes with the three camera views recorded.

The UL marker coordinate information is acquired in Phase II (Figure 2.7b). Only VCR 1 is used in this phase because it is equipped with frame-by-frame advance capability. Each tape is played back and the desired frames of video information are selected. To acquire the coordinates of the centres of the markers, each of the selected frames are frozen and captured. The frozen frame is displayed on the Sony Monitor. This information also goes to the Matrox image processing board to be processed. Here the image is converted from a grey scale image to a binary black and white image which is sent back to the Sony Monitor for display over four lines. Three of the lines are the red, green, and blue segments of the image; the fourth line is the external synchronizing line. The image stored in the image processing board's memory is further processed by the system software to find the centres of the UL markers which can then be stored into a data file.

2.3.3 Calibration Box

In order to calibrate UM²AS (the calibration procedure is presented in the next section) an apparatus is needed in which markers called control balls (CBs) can be placed within the viewing space, with known measured 3-D centroids. A 1m³ calibration box to which the CBs are attached was created from welded square aluminum tubing (Figure 2.8a). Eight CBs are used and these are attached to the box using a C-clamp with a rod welded onto it as shown in Figure 2.8b. This apparatus allows the operator to place the CBs anywhere in the space defined by the calibration box and within the view of all three cameras. The CB can also slide up and down on its rod to allow for more adjustable placement.

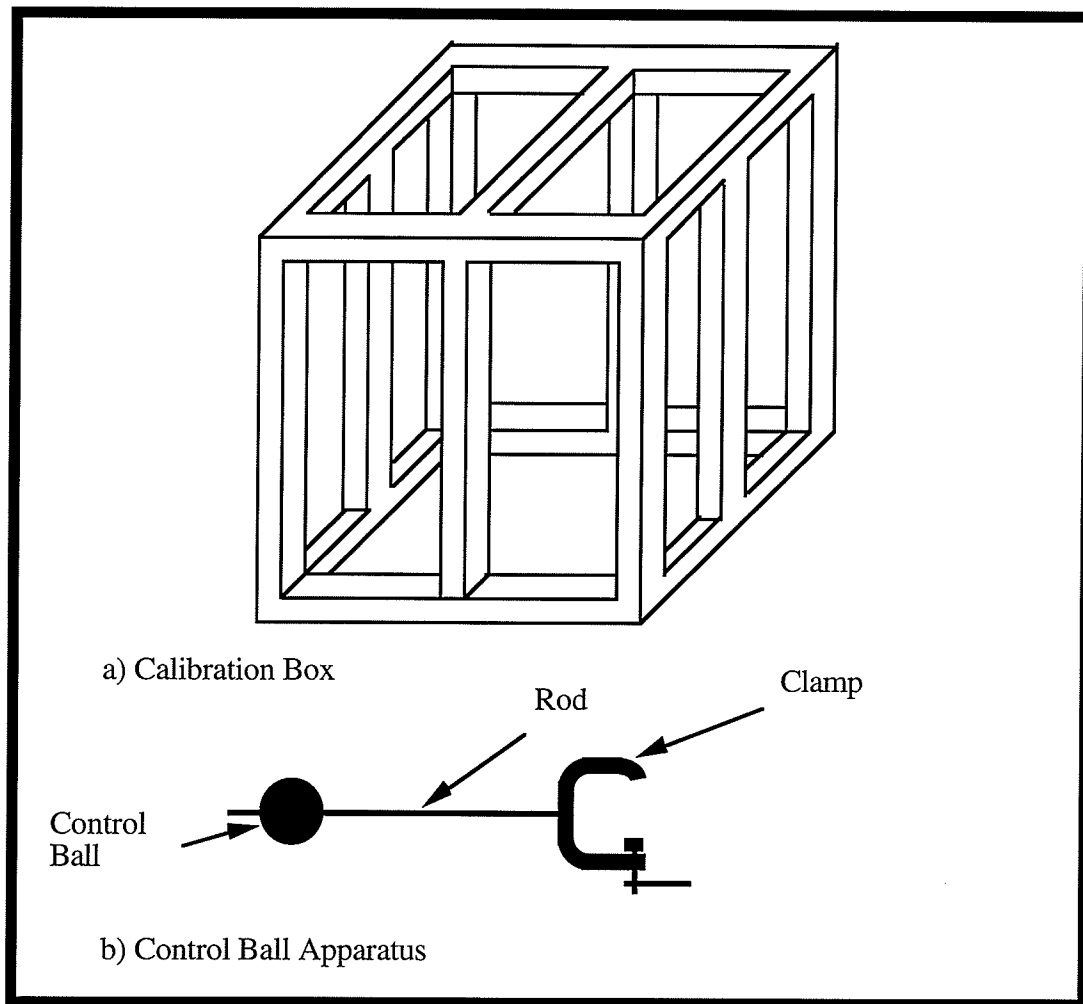


Figure 2.8 Calibration Box and Control Ball Attachment

2.4 Calculating the Upper Limb Real World Marker Coordinates

The current version of UM²AS discussed in this thesis uses three cameras. Using three or more cameras reduces the possibility of UL markers disappearing from the view of two cameras. Viewing the UL marker by at least two cameras is essential to calculate the three dimensional coordinate centre of the UL markers.

UM²AS in essence may be viewed as three two camera systems. Thus the procedure to calculate the UL 3-D centroids is the same as that developed by Safaee-Rad in his thesis for the two camera system [12, pp. 53]. It is repeated in detail in Appendix B and in general here to establish a notation that distinguishes between which camera pairs are being considered. To calculate the eight angular rotations of the UL in any orientation, the real world 3-D centroids of all seven reflective anatomical markers must be calculated. This requires calibration of the cameras. The calibration is essential because it relates the real world 3-D centroids with the 2-D camera view centroids (U_i^k, V_i^k) in a linear fashion. To achieve this, calibration parameters (L_1^k, \dots, L_{11}^k) must be found which will give UM²AS the proper information from which to calculate the 3-D real world marker centroids.

There are 11 calibration parameters (CPs), thus 11 independent equations are needed to solve for them. To acquire 11 independent equations, the information needed is the measured real world 3-D centroids $(X_i^{CB}, Y_i^{CB}, Z_i^{CB})$ and the 2-D camera view centroids (U_i^k, V_i^k) of at least six markers. For the purpose of this project eight known markers called control balls (CBs) were used. Once the real world 3-D centroids and the camera view 2-D centroids of the CBs are known, the CPs can be calculated using equation 2.4 (the derivation of this equation is in Appendix B).

$$\begin{bmatrix} L_1^k \\ L_2^k \\ \vdots \\ L_{10}^k \\ L_{11}^k \end{bmatrix} = (\mathbf{A}^T \mathbf{A})^{-1} \mathbf{A}^T \begin{bmatrix} U_1^k \\ V_1^k \\ U_2^k \\ V_2^k \\ \vdots \\ U_8^k \\ V_8^k \end{bmatrix} \quad (2.4)$$

where

$$\mathbf{A} = \begin{bmatrix} X_1^{CB} & Y_1^{CB} & Z_1^{CB} & 1 & 0 & 0 & 0 & 0 & -U_1^k X_1^{CB} & -U_1^k Y_1^{CB} & -U_1^k Z_1^{CB} \\ 0 & 0 & 0 & 0 & X_1^{CB} & Y_1^{CB} & Z_1^{CB} & 1 & -V_1^k X_1^{CB} & -V_1^k Y_1^{CB} & -V_1^k Z_1^{CB} \\ X_2^{CB} & Y_2^{CB} & Z_2^{CB} & 1 & 0 & 0 & 0 & 0 & -U_2^k X_2^{CB} & -U_2^k Y_2^{CB} & -U_2^k Z_2^{CB} \\ 0 & 0 & 0 & 0 & X_2^{CB} & Y_2^{CB} & Z_2^{CB} & 1 & -V_2^k X_2^{CB} & -V_2^k Y_2^{CB} & -V_2^k Z_2^{CB} \\ \vdots & \vdots \\ X_8^{CB} & Y_8^{CB} & Z_8^{CB} & 1 & 0 & 0 & 0 & 0 & -U_8^k X_8^{CB} & -U_8^k Y_8^{CB} & -U_8^k Z_8^{CB} \\ 0 & 0 & 0 & 0 & X_8^{CB} & Y_8^{CB} & Z_8^{CB} & 1 & -V_8^k X_8^{CB} & -V_8^k Y_8^{CB} & -V_8^k Z_8^{CB} \end{bmatrix}$$

- $(\mathbf{A}^T \mathbf{A})^{-1} \mathbf{A}^T$ - pseudo inverse of \mathbf{A} [13]
- (L_1^k, \dots, L_{11}^k) - eleven calibration parameters for camera k
- $(X_i^{CB}, Y_i^{CB}, Z_i^{CB})$ - tape measured real world 3-D CB centroid i
- (U_i^k, V_i^k) - 2-D camera view centroid i for camera k

The calibration parameters (CPs) $((L_1^n, \dots, L_{11}^n)$ and (L_1^m, \dots, L_{11}^m)) and the 2-D UL camera view centroids from at least two different camera views $((U_i^n, V_i^n)$ and (U_i^m, V_i^m)) are then used to calculate the 3-D real world centroids of the UL markers $((X_i^{mn}, Y_i^{mn}, Z_i^{mn}))$. This is done using Equation 2.5 which is also derived in Appendix B.

$$\begin{bmatrix} X_i^{mn} \\ Y_i^{mn} \\ Z_i^{mn} \end{bmatrix} = (\mathbf{B}^T \mathbf{B})^{-1} \mathbf{B}^T \begin{bmatrix} U_i^m - L_4^m \\ V_i^m - L_8^m \\ U_i^n - L_4^n \\ V_i^n - L_8^n \end{bmatrix} \quad (2.5)$$

Where

$$\mathbf{B} = \begin{bmatrix} L_1^m - L_9^m U_i^m & L_5^m - L_9^m V_i^m & L_1^n - L_{9n} U_i^n & L_5^n - L_9^n V_i^n \\ L_2^m - L_{10}^m U_i^m & L_6^m - L_{10}^m V_i^m & L_2^n - L_{10n} U_i^n & L_6^n - L_{10n} V_i^n \\ L_3^m - L_{11}^m U_i^m & L_7^m - L_{11}^m V_i^m & L_3^n - L_{11n} U_i^n & L_7^n - L_{11n} V_i^n \end{bmatrix}^T$$

- $(\mathbf{B}^T \mathbf{B})^{-1} \mathbf{B}^T$ - the pseudo inverse of \mathbf{B} [13]
- (L_1^n, \dots, L_{11}^n) - CPs for camera \mathbf{n}
- (U_i^n, V_i^n) - 2-D centroid for UL marker \mathbf{i} from camera view \mathbf{n}
- (L_1^m, \dots, L_{11}^m) - CPs for camera \mathbf{m}
- (U_i^m, V_i^m) - 2-D centroid for UL marker \mathbf{i} from camera view \mathbf{m}
- $(X_i^{mn}, Y_i^{mn}, Z_i^{mn})$ - 3-D calculated real world marker \mathbf{i} centroid, calculated from camera \mathbf{m} and \mathbf{n} ($\mathbf{m} \neq \mathbf{n}$)

Three cameras are used to reduce the possibility that an anatomical marker leaves the view of any two cameras. A three camera system, using Equation 2.5, yields three different three-dimensional coordinates for each marker. The three possible combinations are $(X_i^{12}, Y_i^{12}, Z_i^{12})$, $(X_i^{13}, Y_i^{13}, Z_i^{13})$, and $(X_i^{23}, Y_i^{23}, Z_i^{23})$. Three possible situations that could arise are: 1) a marker is present in all three camera views, 2) a marker is not seen in the view of one camera, and 3) a marker is not seen in the view of two or three of the

cameras.

If the marker is missing in two or three camera views not enough information will be available to calculate the three dimensional real world marker centre, therefore the coordinates are set to 999 as in Equation 2.6.

$$(X_i^{avg}, Y_i^{avg}, Z_i^{avg}) = (999, 999, 999) \quad (2.6)$$

If the marker is missing in only one camera view, $(X_i^{avg}, Y_i^{avg}, Z_i^{avg})$ is set to the value calculated by the other two cameras. For example if the marker is not present in camera 1 then the real world coordinate is given by Equation 2.7.

$$(X_i^{avg}, Y_i^{avg}, Z_i^{avg}) = (X_i^{23}, Y_i^{23}, Z_i^{23}) \quad (2.7)$$

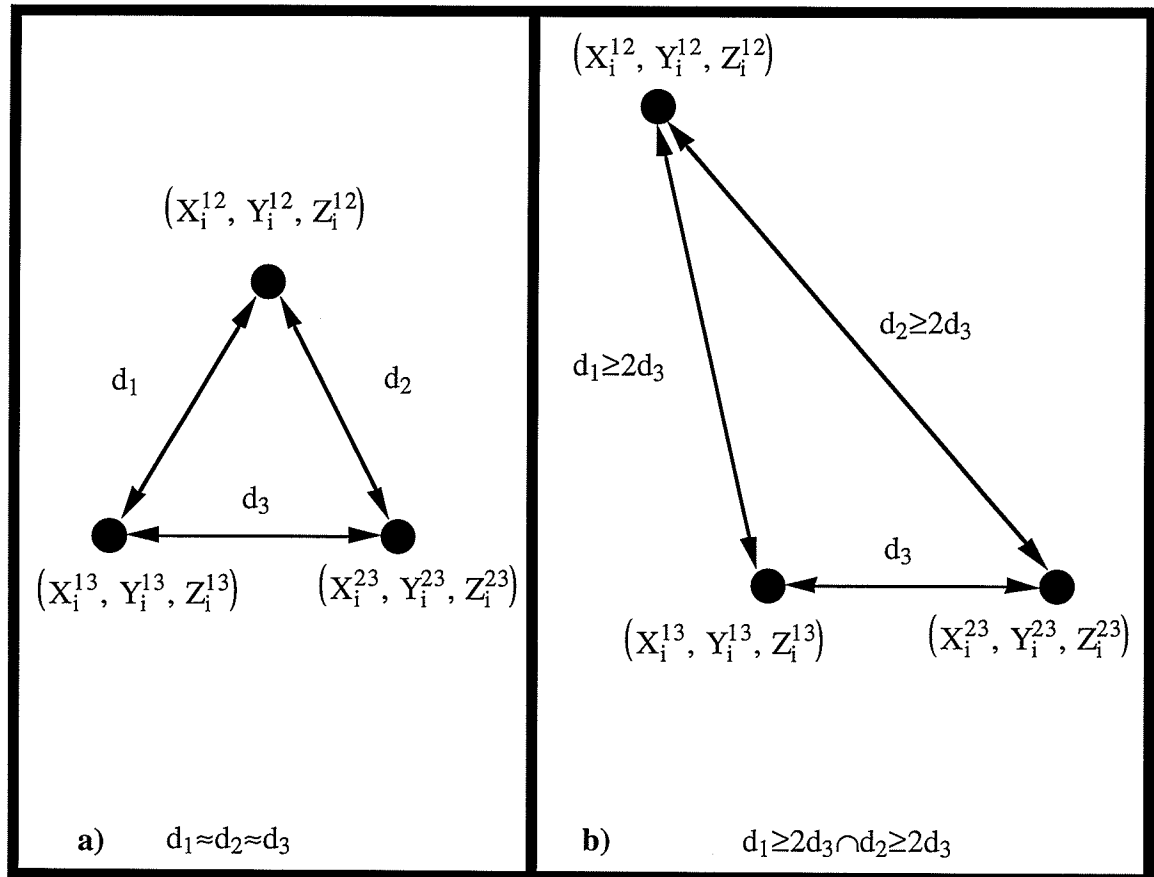


Figure 2.9 Criterion for Choosing between Three Calculated Points

The final case is when the marker is present in all three views. When this occurs three possible three dimensional positions for the marker are generated. The question is, which one is correct? To answer this, a euclidean distance measure is used. The criterion used is to use all three markers if they are an equal euclidean distance from each other. If this is not the case, then exclude one of the calculated points if it is twice as far away from the other two points as they are from each other (Figure 2.9). For example, if the distance d_1 and d_2 are twice that of d_3 ($d_1 \geq 2d_3 \cap d_2 \geq 2d_3$) then the calculated value $(X_i^{12}, Y_i^{12}, Z_i^{12})$ is left out of the calculation as given by

$$(X_i^{avg}, Y_i^{avg}, Z_i^{avg}) = \left(\frac{X_i^{13} + X_i^{23}}{2}, \frac{Y_i^{13} + Y_i^{23}}{2}, \frac{Z_i^{13} + Z_i^{23}}{2} \right). \quad (2.8)$$

Note that the twice as far threshold could be any number, therefore with more experimentation and data a better threshold might be found.

CHAPTER III

Software Design and Development

This chapter describes the software design and development that links the mathematics and equipment of the University of Manitoba Motion Analysis System (UM²AS) described in Chapter II. An environment is created that is suitable for an operator using UM²AS in a clinical environment.

3.1 The Overall Program

The overall program is that shown in block diagram form in Figure 3.1. The program consists of four main sections which are: a) *Marker Coordinate Digitizing*, b) *Calibration Parameters*, c) *X,Y, and Z Coordinate Calculation*, and d) *Calculate Euler Angles*. The *Marker Coordinate Digitizing* section allows the operator to digitize the 2-D upper limb (UL) camera view marker centroids for a specified number of frames from one of the cameras. This data is then stored to a file with the file extension of da1 (camera 1), da2 (camera 2), or da3 (camera 3). The *Calibration Parameters* section first allows the operator to digitize the 2-D camera view centroids of the control balls (CBs) for camera 1. It then uses a file with the tape measured real world 3-D CB marker centroids (*.msr) and the 2-D CB camera view centroids to calculate the calibration parameters (CPs) for camera 1 and stores them in a file (*.cp1). This process is then repeated for camera one and two and the results are respectively stored in the files *.cp2 and *.cp3. The *X,Y, and Z Coordinate Calculation* section takes the 2-D camera view UL centroids and the CPs from all three cameras to calculate the 3-D real world UL marker centroids which are then stored to a file (*.tdc). The *Calculate Euler Angles* section uses the calculated 3-D real world UL centroids to calculate the Euler angles for the shoulder, elbow, and wrist and stores them in

selected files with the extensions respectively shd, elb, and wst.

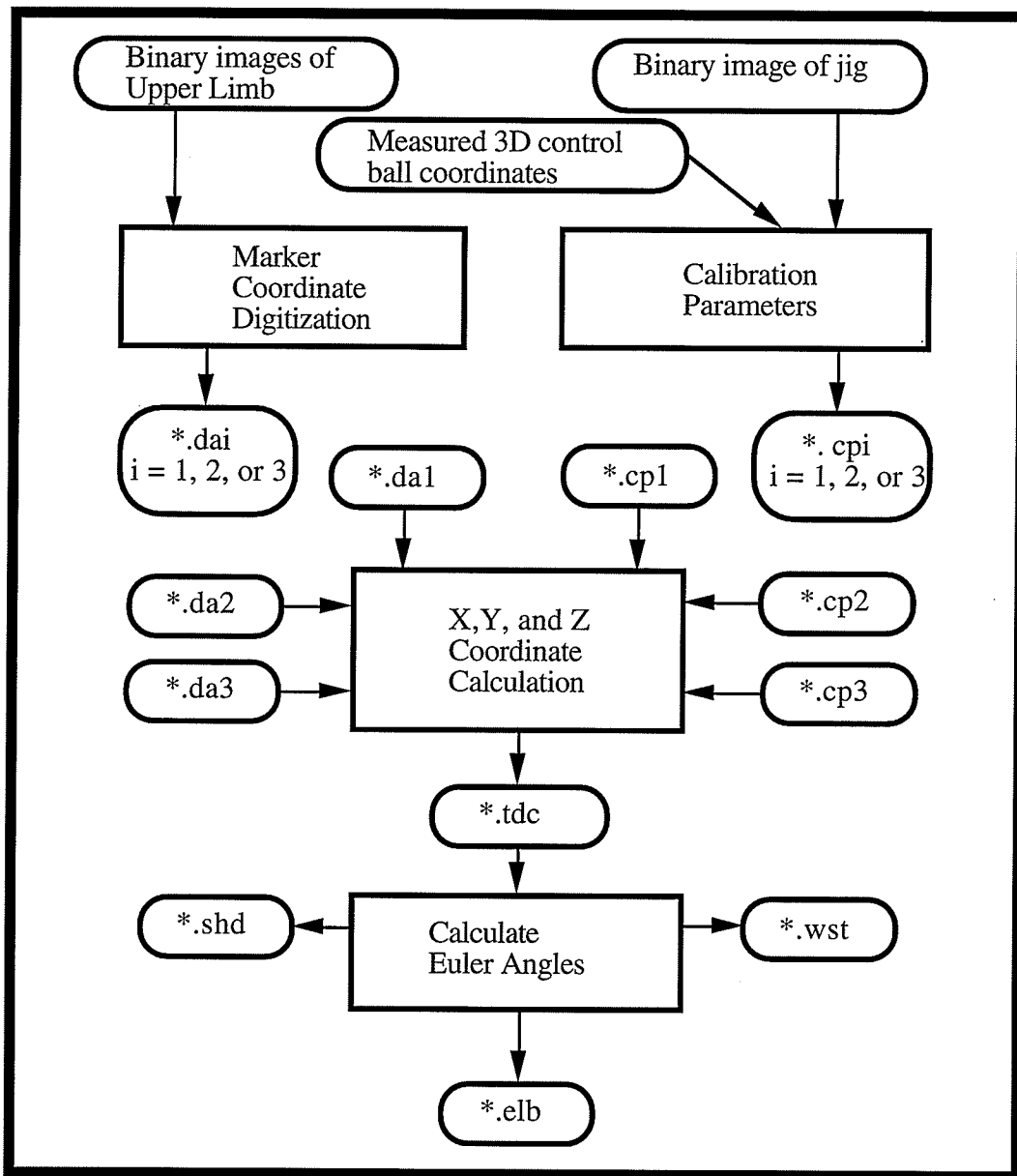


Figure 3.1 Block Diagram of Complete Program

3.2 Design Criteria

UM²AS software was designed with the operator in mind. The main criteria for most operators are that the system be pleasing to work with, can be used by operators with minimal computer skills, and option parameters can be easily changed. Using these criteria, UM²AS software was designed to use a pop up window, integrated environment as illustrated in Figure 3.2.

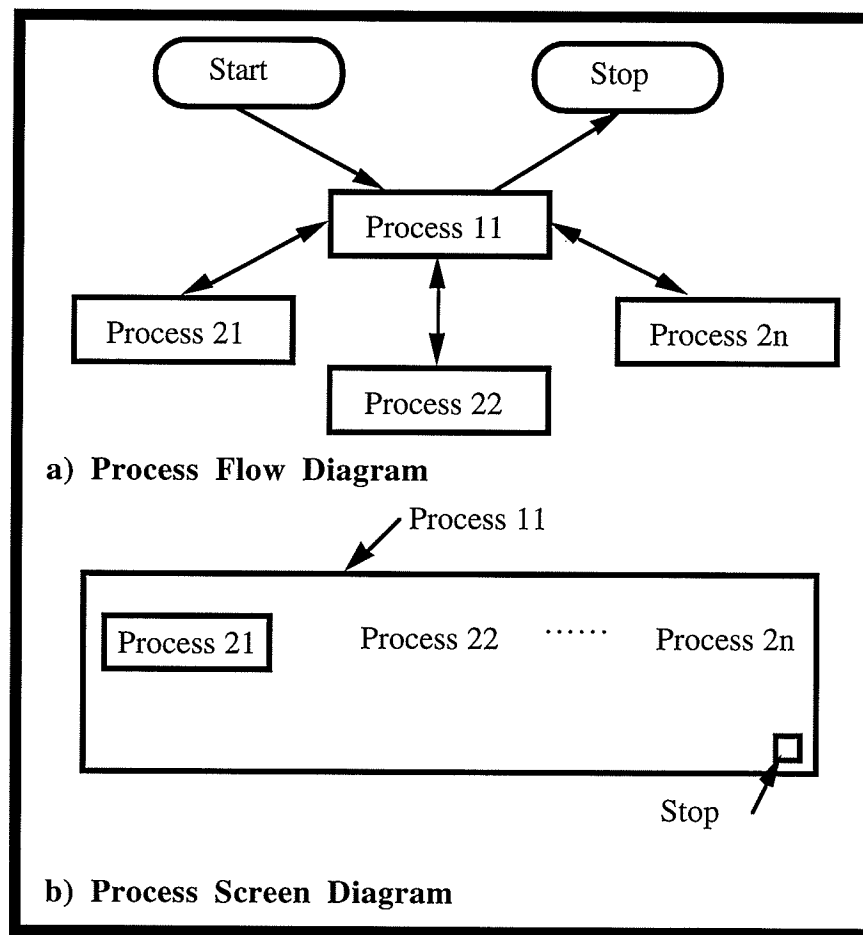


Figure 3.2 Flow Structure of The Program

Upon starting the program, the operator has moved to process 11 (Figure 3.2a). This is usually a menu with more options (Figure 3.2b) known here as Process 21, Process 22, and up to Process 2n. For example, one could now enter the highlighted

Process 21. This process could be more options or a specific task such as entering a file name, setting program parameters, or displaying data. To enter one of the other processes, one must first return to the level above (in this case Process 11) by either clicking the mouse button in the little square box located in the bottom right hand corner of the Process 21 window or by pressing the escape key (assuming Process 21 is more options). To exit the program, the operator must always return to Process 11 first and then either exit by clicking the left mouse button in the little square box located at the bottom right hand corner of the Process 11 window or by pressing the escape key. The program was designed this way to simplify the programming, conserve working RAM, and to allow the operator to visit processes many times until all the actions of the program are performed properly.

3.3 Main Menu for the Integrated Environment

The main menu of the system can be seen in the box at the top of Figure 3.3 and can be thought of as Process 11. By using either the mouse or key board commands the program operator can go into either the *Camera Information* or *Data Calculation* option of the program. The *Camera Information* option allows the operator to acquire the camera

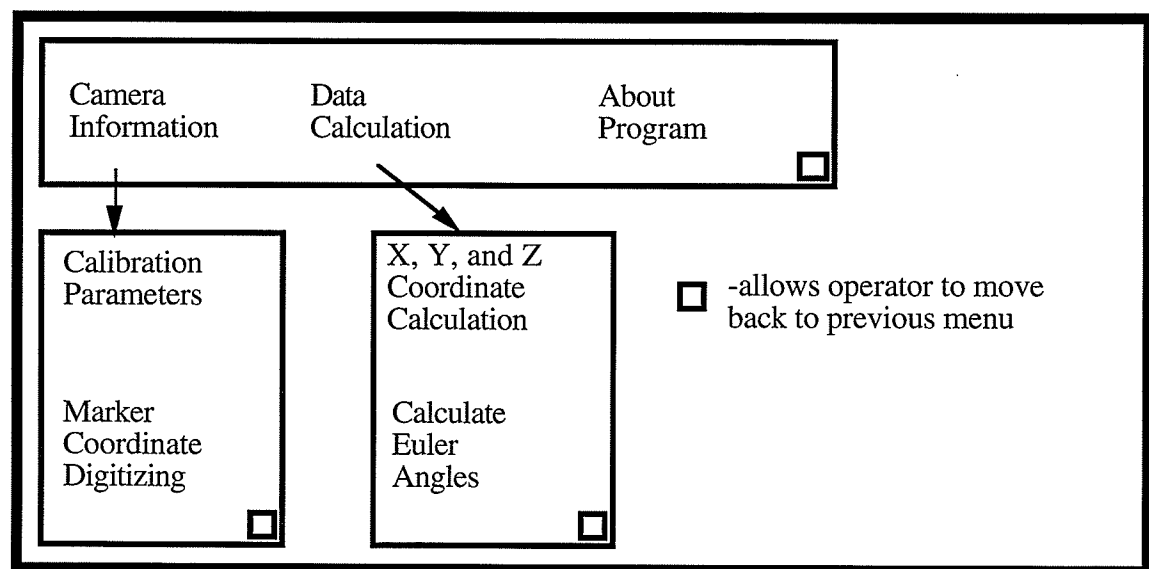


Figure 3.3 Main Menu of the Program

calibration parameters (L_1^k, \dots, L_{11}^k) or the 2-D camera view centroids (U_i^k, V_i^k) of the UL markers. The *Data Calculation* option is used to calculate either the 3-D real world centroids $(X_i^{avg}, Y_i^{avg}, Z_i^{avg})$ of the UL markers or the Euler angles of the shoulder $(\phi_1, \theta_1, \psi_1)$, elbow (ϕ_2, ψ_2) , and wrist $(\phi_3, \theta_3, \psi_3)$.

3.4 Calculating Camera Calibration Parameters

The calibration procedure used is to first measure the 3-D real world centroids of the eight control balls (CBs) and then record the three camera views of the calibration jig onto beta tape. Each camera view is then processed to gather the 2-D CB camera view centroids. Lastly the calibration parameters (CPs) are calculated using the 3-D tape measured

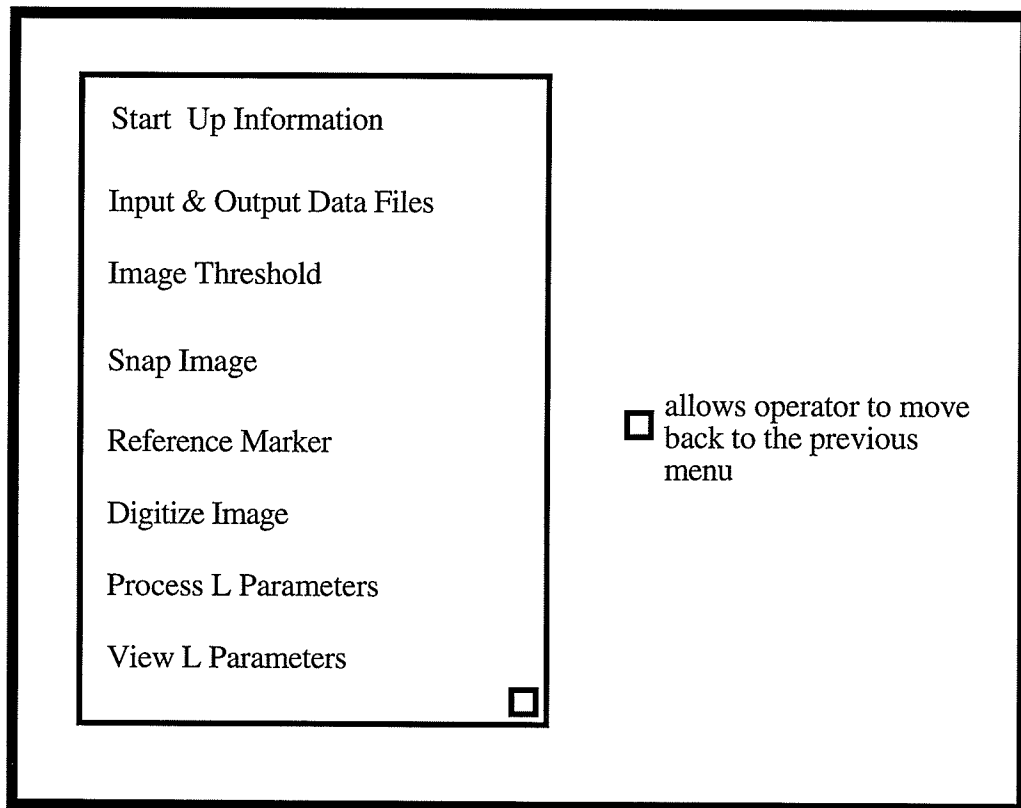


Figure 3.4 Calibration Parameter Calculation

CB centroids and their camera view centroids. This procedure can be carried out using the calibration parameters menu shown in Figure 3.4.

The input file needed is the *.msr file which contains the measured real world centroids $(X_i^{CB}, Y_i^{CB}, Z_i^{CB})$ of the eight control balls. The centroids are entered into the file with a text editor, each on a separate line starting with CB 1. The output file (*.cp1, *.cp2, or *.cp3 for camera one, two, or three respectively) generated by the software contains the calibration parameters (CPs), each on a separate line starting with parameter 1. Typical *.msr and *.cp1 files are shown in Figure 3.5. The current date is also stored to *.cp1 but not to *.cp2 or *.cp3. This lets the operator know when the calibration files were created. To calculate the CPs successfully the operator must perform the eight tasks shown in Figure 3.4; *Start Up Information, Input*

72.2	40.5	-6.4	YEAR: 92 MONTH: 11 DAY: 27
60.0	31.8	31.5	-0.7230327
63.6	5.8	59.5	3.6617928
46.8	16.8	-7.5	0.0439470
21.0	5.7	73.9	115.3470764
13.7	46.7	37.8	-0.7258390
48.3	72.3	62.2	0.1574676
32.5	31.2	58.9	-4.1144953
			395.9822693
			-0.0029378
			0.0008468
			-0.0003879
a) Typical *.msr			b) Typical *.cp1

Figure 3.5 Contents of *.msr and *.cp1

& *Output Data Files, Image Threshold, Snap Image, Reference Marker, Digitize Image, Process L Parameters, and View L Parameters*. The objective of the CPs option is to calculate the 11 CPs.

The *Start Up Information* option (Figure 3.6) prompts the operator to set processing flags which are: camera the data are from, the date, and threshold type (inverted - black

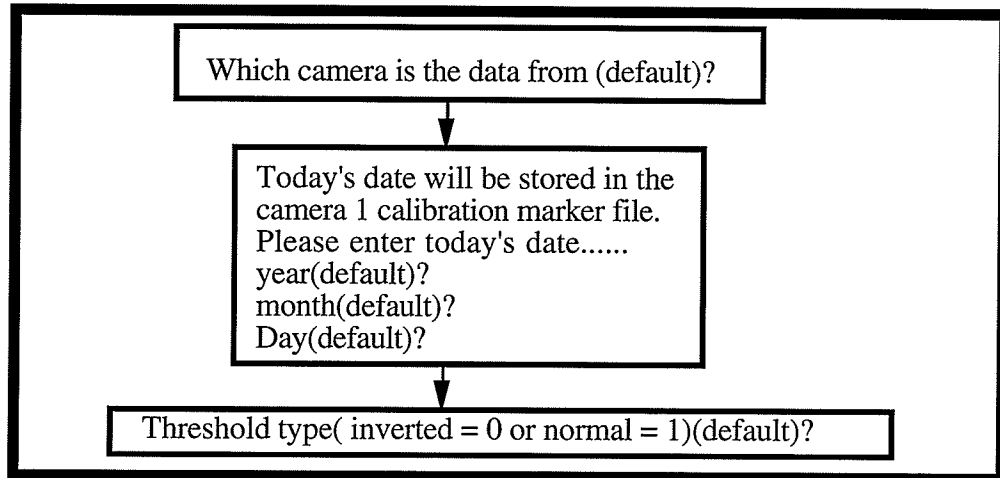


Figure 3.6 Calibration Parameters Start Up Information Option

markers on a white background, normal - white markers on a black background). The default for the date is that of the DOS clock. The camera default is 1 and the threshold type is initially set to "normal" or 1. Upon completion of setting this series of dialog boxes, the operator is automatically brought back to the *Calibration Parameters* menu. If data from cameras other than number one are being processed, the date option box does not appear.

As shown in Figure 3.7a, the *Input & Output Files* option allows the operator to input the name of the file that has the relevant measured 3-D control ball centroids $(X_i^{CB}, Y_i^{CB}, Z_i^{CB})$ for the calibration frame (**.msr*) and the name of the file in which to store the calibration parameters (**.cp1*, **.cp2*, or **.cp3* for camera one, two, or three respectively). This can be done either by manually typing the file names or by using the mouse to select the file name from a list in the current directory (Figure 3.7b).

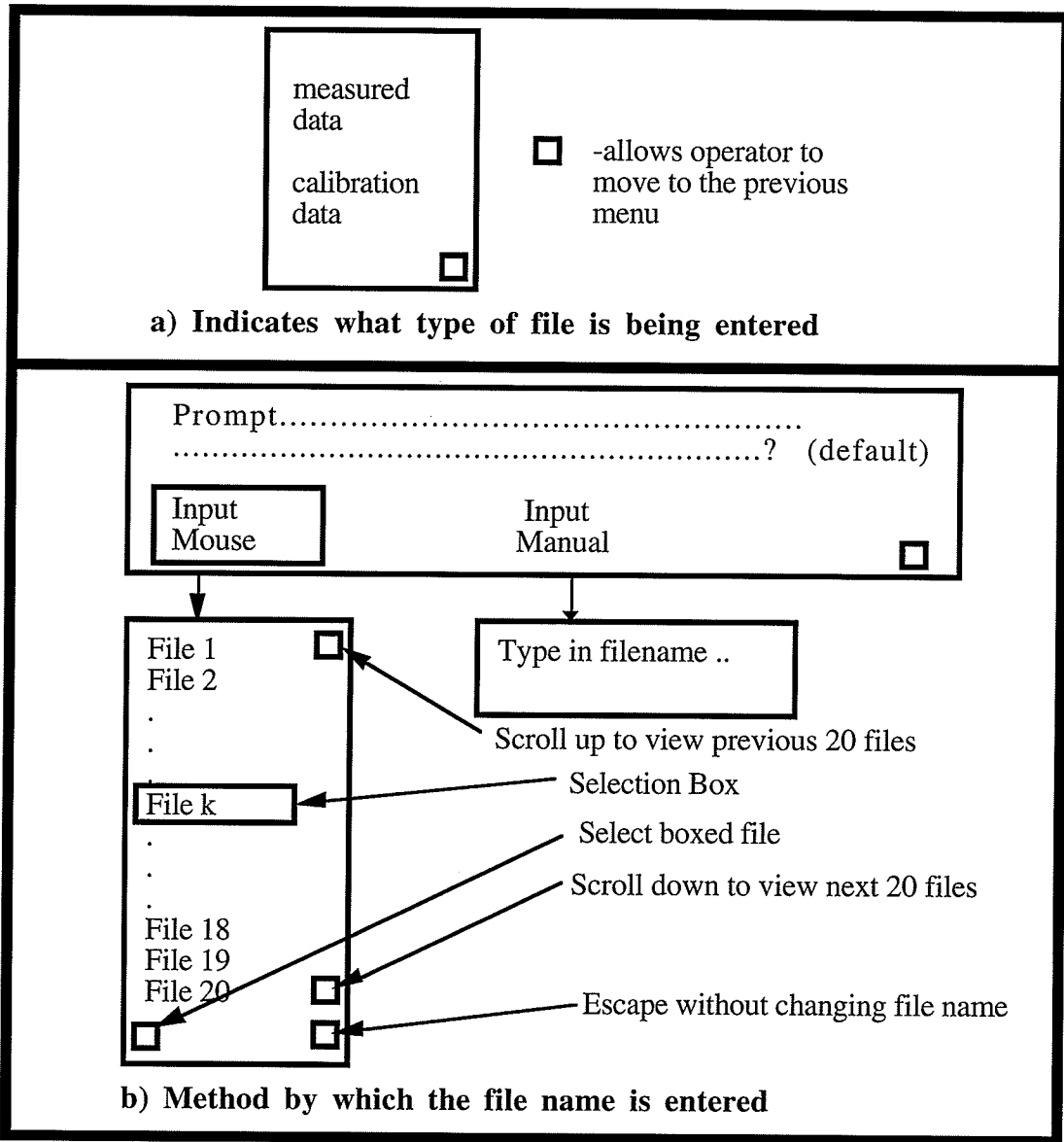


Figure 3.7 Calibration and Measured Data File Name Selection

In the *Image Threshold* option (Figure 3.8), the operator selects a value that transforms the normal grey scale into a binary scale. For example, if a threshold value of 51 is chosen then the original grey scale will be mapped as in Figure 3.8a. Every pixel with a grey scale below 51 will be set to zero or black and every pixel with a grey scale above and including 51 will be changed to 253 or white. Thus a binary image is created from the original. The dialog box that appears for this option in the program is shown in Figure 3.8b.

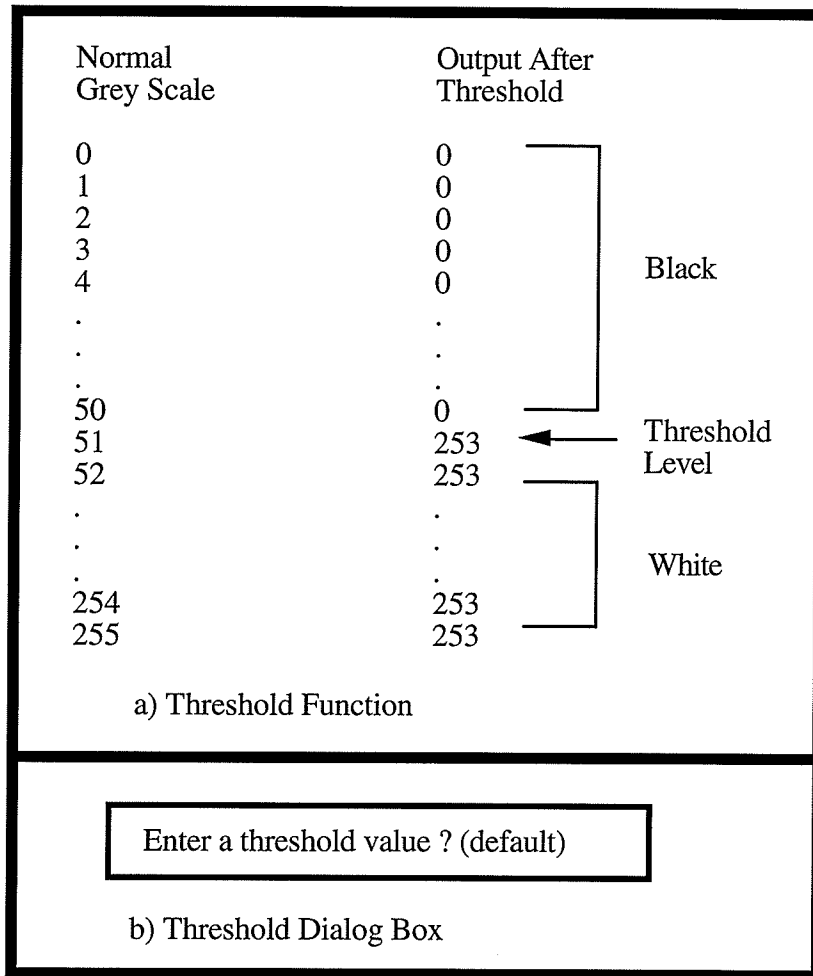


Figure 3.8 Threshold Function and Dialog Box

The *Snap Image* option allows the operator to select a grey scale image from the VCR and process it into a binary image. The image is then stored in the memory of the PIP image processing board to be processed further.

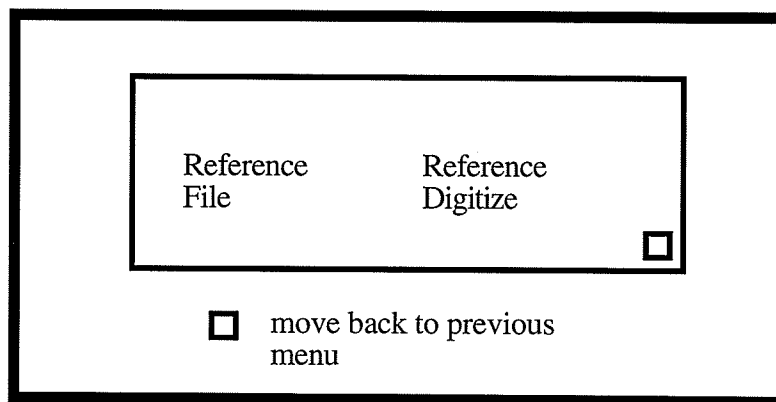


Figure 3.9 Reference Marker Acquisition Menu

The *Reference Marker* option allows the program operator to acquire the reference marker coordinate data either from a pre existing file (*.rf1, *.rf2, or *.rf3 for camera one, two, or three respectively) or by digitizing the marker from a binary image (Figure 3.9).

The file selection method is the same as that shown in Figure 3.7b. The second option *Reference Digitize*, switches the cursor to the image processing board's monitor to allow the operator to select the reference marker in the binary image. After the reference marker has been chosen the cursor is brought back to the computer screen ready for the operator's next choice.

The *Digitize Image* portion of the program allows the operator to acquire the 2-D camera view centroids of the eight control balls (U_i^k, V_i^k) . Figure 3.10 shows the flow chart of this process. The boxes with the black text represent dialog boxes that appear on the computer monitor while the boxes with the white text represent key processes that are imperceptible to the operator. After execution of this section, the cursor is transferred to the image processing board's monitor (Sony Monitor in this case). The operator is then prompted to place the cursor over a white pixel of marker i and then presses the mouse button to digitize marker i . The program uses this information to calculate the centroid of marker i . This process is continued until all eight control balls and the reference marker in camera view k are selected. The control balls must be selected in ascending order from control ball one to eight. Upon completion the operator is returned to the main calibration menu and the cursor is returned to the computer monitor for selection of the next operation from the menu.

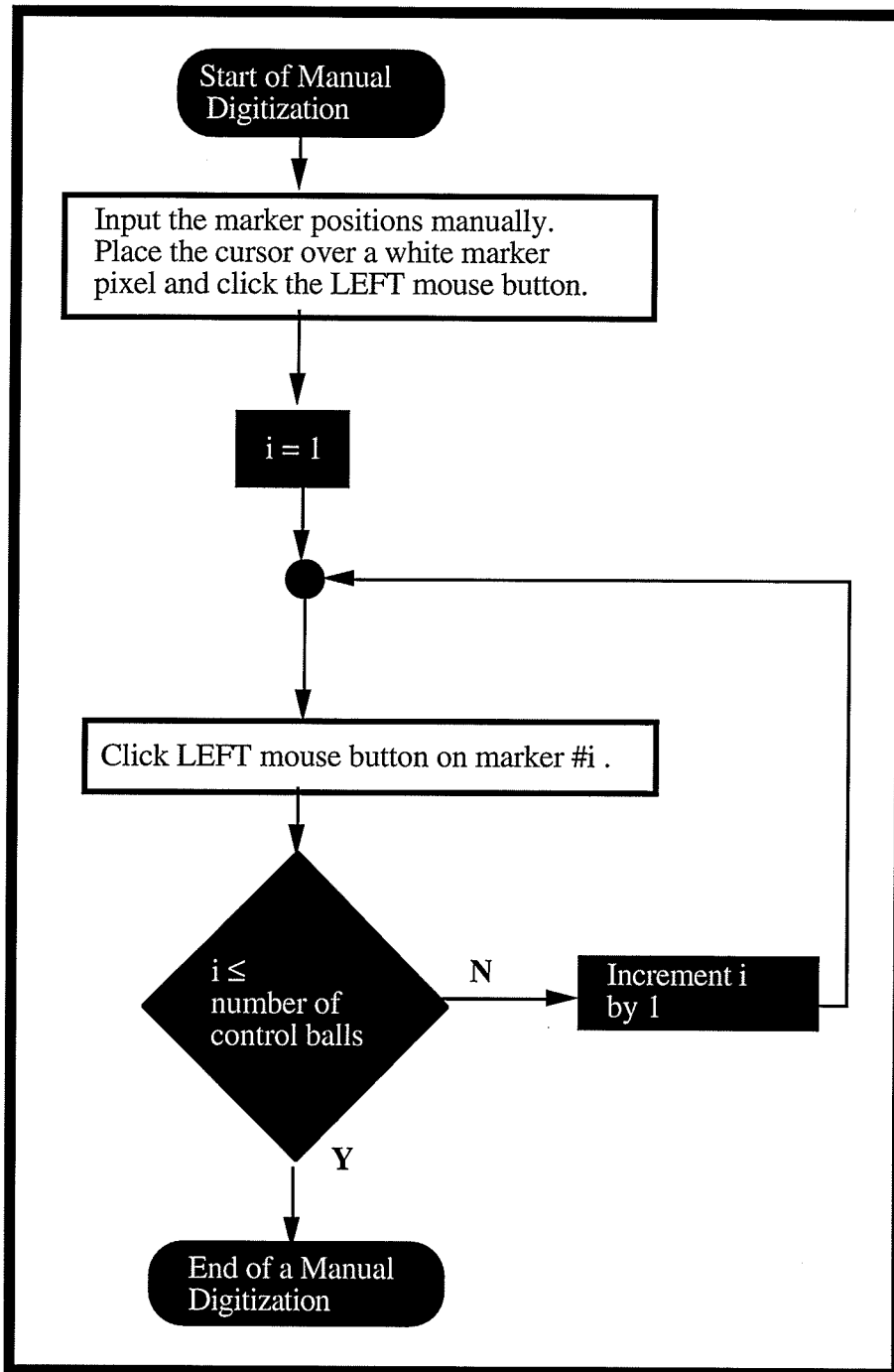


Figure 3.10 Manual Digitization Flow Chart

The *Processing L Parameters* option takes the digitized centroids of the control balls from camera k and the 3-D measured control ball coordinates $(X_i^{CB}, Y_i^{CB}, Z_i^{CB})$ from the *.msr file and uses the linear algebra discussed in Section 2.4 to calculate the calibration parameters $(L_1^k, \dots, L_{i_1}^k)$. These parameters are then saved to a file (*.cp1, *.cp2, or *.cp3

for camera one, two, or three respectively). The *View L Parameters* option allows the operator to view the calculated parameters before exiting the *Calculating Parameters* option. The operator can repeat steps in the *Calculating Parameters* option to verify that the calculated parameters are accurate.

3.5 Marker Coordinate Digitizing

This menu option (Figure 3.11) is used to acquire the 2-D body marker centroids from individual frames of the video tape. This option allows the operator to create a file that contains the 2-D camera view centroids for the motion being studied. A typical format of the file is given in Figure 3.12.

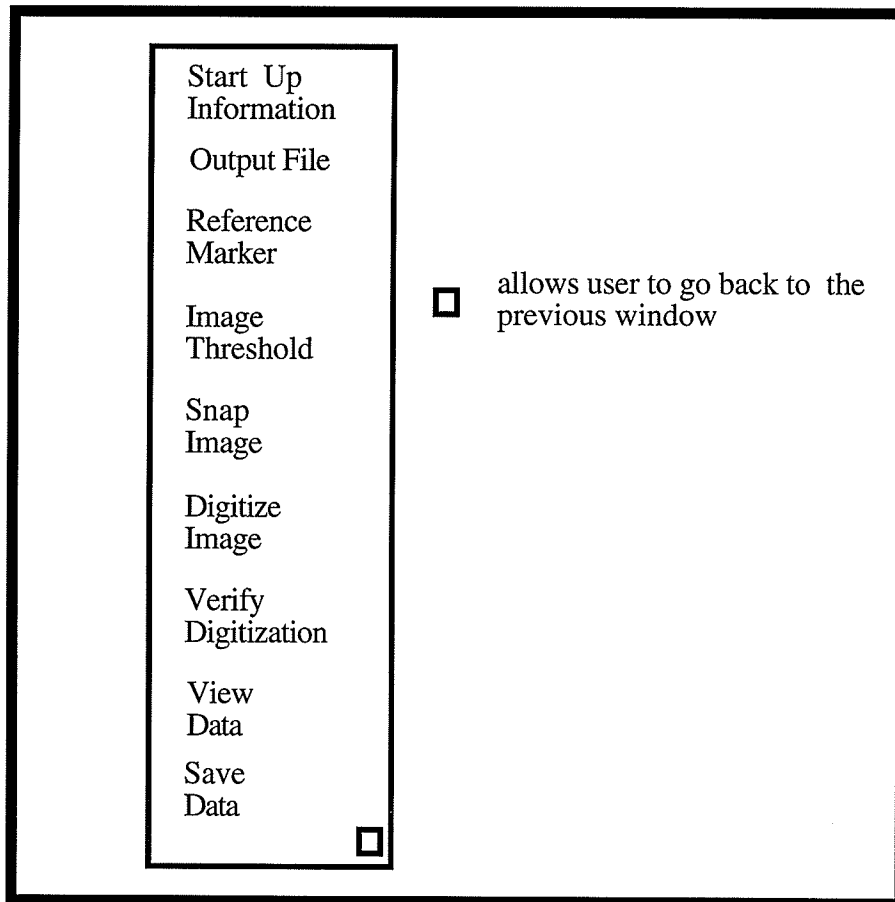


Figure 3.11 Motion Data Acquisition Main Menu

This file is from camera one because it possesses the header (first line) that tells the operator and the program how many frames of information are in the file and how many markers per frame, this header is not part of the camera two or camera three. This particular file contains 10 markers per frame and 2 frames of data.

The values in the file range from 0-511 units for the U and V components. Note that the value 999 also appears for the U and V component. This value represents a marker that could not be seen in the camera's view ($(U_i^k, V_i^k) = (999, 999)$). The options *Reference Marker*, *Image Threshold*, and *Snap Image* perform the same function as in the *Calibration Parameters* option, therefore they are not discussed here.

Number of frames: 2 Number of markers: 10	
262.8384705	137.0000000
255.8384705	185.0000000
266.3038025	234.7425690
291.9871826	370.3589783
367.8384705	413.0000000
327.9577332	382.7706299
368.8384705	410.0000000
999	999
148.5855255	164.1882324
124.2303619	404.0540466
260.7773438	135.8426514
254.7773438	185.8426514
266.5260010	234.1314240
293.1466675	369.5812988
368.7773438	406.8426514
327.9036560	382.0321350
370.7773438	406.8426514
999	999
148.2273407	164.2426453
124.4979324	404.2544250

Figure 3.12 Format of a Camera 1 data file (*.da1)

In principle the *Start Up Information* menu option (Figure 3.13) serves the same purpose as that of the same name in the *Calibration Parameters* option except that there are some additional processing flags to be discussed. The "Last frame to be processed" prompt allows the operator to specify the number of frames to be processed; when this number is

reached the program's frame counter sends a message to the computer monitor and a tone sounds to alert the operator. The "Number of markers" prompt lets the operator specify how many markers are to be digitized per frame (this also includes the reference marker). Currently the largest number of markers allowed is set to 30. The "camera number" prompt allows the operator to tell the program from which camera the markers are to be digitized. Setting the camera number to one causes information about the number of frames and markers to be written to the output file *.da1. The "Number of frames skipped" prompt allows the operator to set the sampling rate. For example choosing one causes the program to sample 30 frames per second.

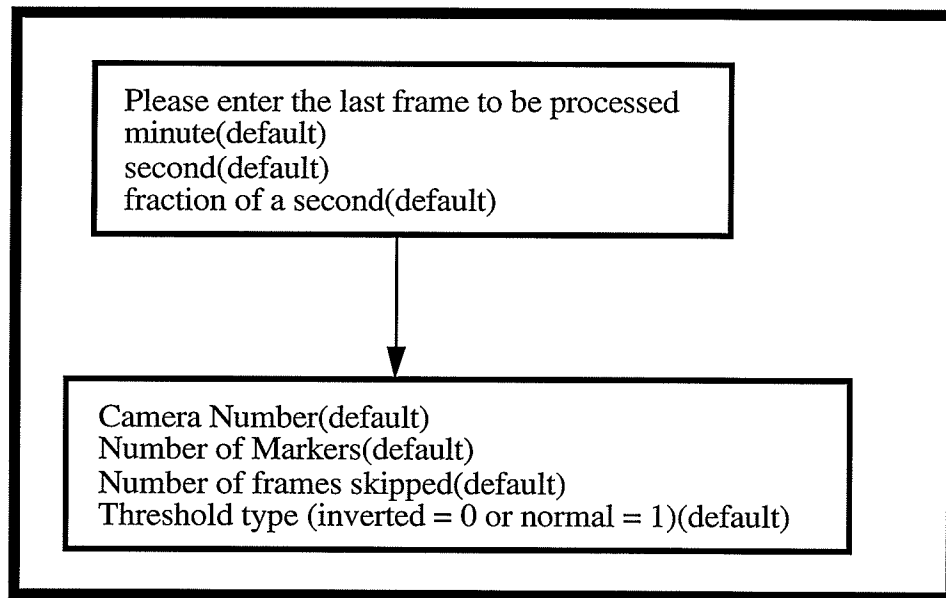


Figure 3.13 Start Up Information for Motion Data Acquisition

The *Output File* option allows the operator to specify the file in which the marker motion data from camera k are to be stored. The file name usually has the form *.dak, where k is the camera number. The file name is entered in the same manner as that described in Figure 3.5 b.

The *Digitize Image* Option lets the operator manually digitize the first two frames using the same algorithm as in the *Calibration Parameters* option (Figure 3.8) with the

exception of two changes. The first is changing the condition "number of control balls" to "the number of markers". The second change is that a box is placed in the right upper corner of the image processing board's monitor. Clicking the mouse in this box tells the program that a marker *i* is not present on the screen. Marker *i* will then have its coordinates set to (999,999).

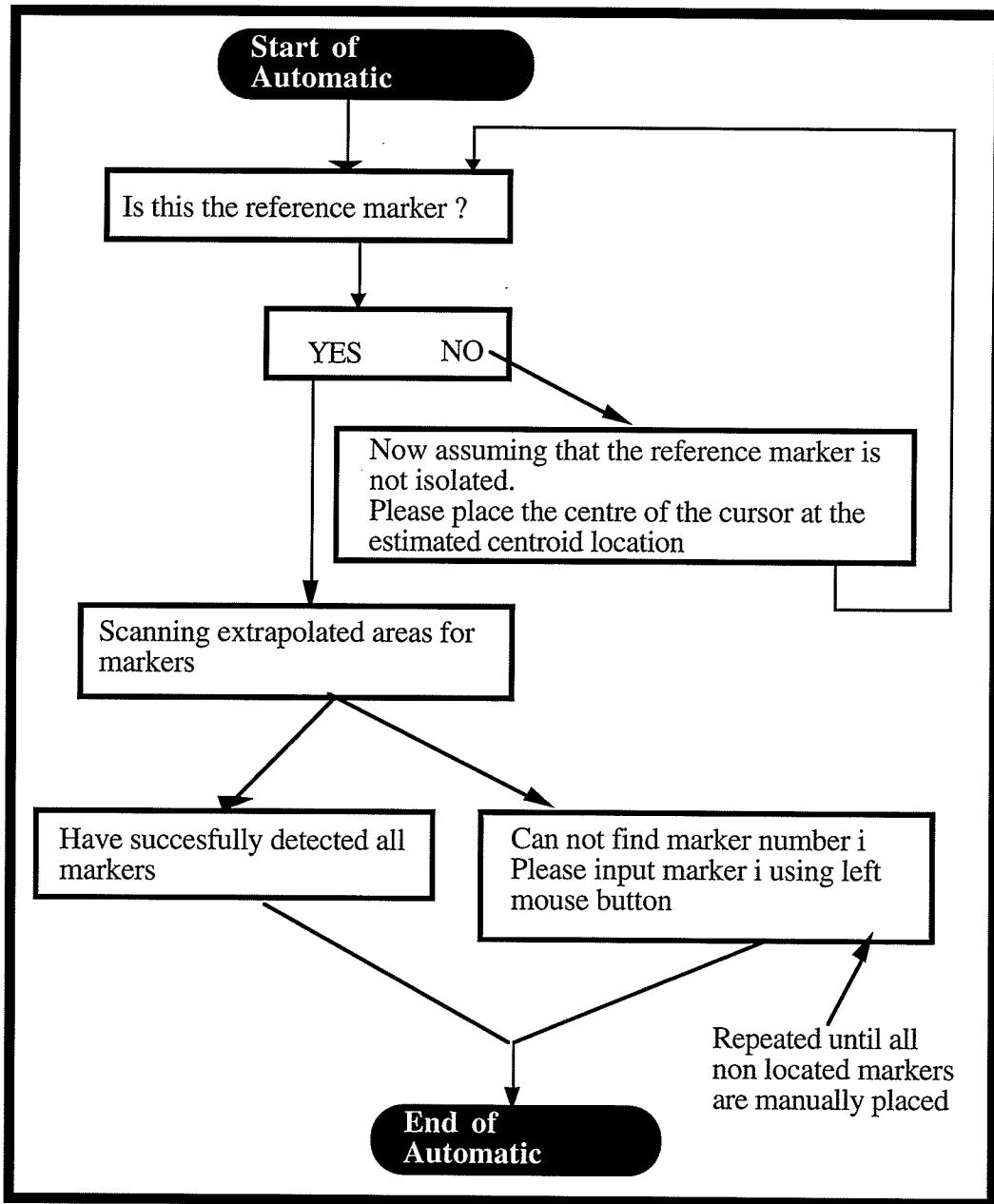


Figure 3.14 Automatic Digitization Flow Chart

After completing the second frame the operator is automatically switched to an automatic digitization mode in which the coordinates of the camera view (U_i^k, V_i^k) body markers from the previous two frames are used to extrapolate their location in the current frame (Figure 3.14). The first step in Figure 3.14 is the location of the reference marker. The program finds the reference marker for that frame by searching the portion of the image board screen specified by the constant reference marker centroid. The program scans around this centroid in a 5x5 grid for a white pixel that is a portion of the reference marker. If white pixels are encountered in this area the operator is asked to verify that this is the reference marker by selecting "YES" or "NO" from the menu. If the answer is "NO", the program allows the operator to manually digitize the marker that represents the reference marker. After this is done the program asks again for confirmation that this is the reference marker. If the answer is "YES", the program linearly extrapolates the location of the body markers using information from the previous two frames. It then scans the area around these centroids for white pixels that represent a marker in a 5x5 grid. If a white pixel is not found this grid is expanded up to a factor of 10 before terminating the search. At this point, the program has either a) found all the markers or b) had difficulty in finding some or all of the markers. If all markers are found, the program returns the message "Have successfully detected all markers". If it cannot find all the markers, the operator is asked to manually digitize those not located. This ends the automatic marker detection. If an error has been made in manual or automatic location of the markers it can be corrected by using the *Verify Digitization* option.

The *Verify Digitization* option (Figure 3.15) allows correction of the body marker coordinates if the marker centroid was calculated incorrectly in the *Digitize Image* option. The program first regenerates the image processing board screen and then asks the operator to verify, in sequence, the marker positions starting with marker 1. If the marker position is correct the operator selects "YES". The program moves to the next marker where the process is repeated. If "NO" is chosen the cursor is switched to the image processing

3.6 Real World (X, Y, Z) Coordinate Calculation

This section allows the operator to calculate the 3-D upper limb centroids $(X_i^{avg}, Y_i^{avg}, Z_i^{avg})$ using the calibration parameters (L_1^k, \dots, L_{11}^k) and the 2-D camera view UL centroids (U_i^k, V_i^k) from two or three cameras (Figure 3.16). Input files needed to calculate the 3-D centroids are two or three of the calibration files (*.cp1, *.cp2, and *.cp3) and two or three of the motion data camera view files (*.da1, *.da2, and *.da3). The menu option to perform this calculation is shown in Figure 3.16. An example of the output file used to store the calculated X, Y, and Z real world coordinates (*.tdc) is shown in Figure 3.17.

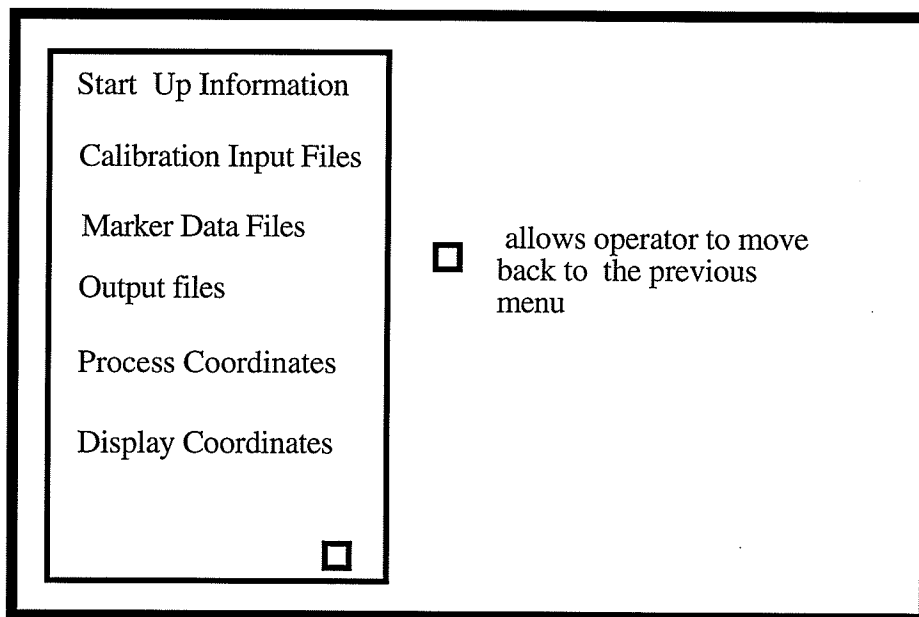


Figure 3.16 Menu for X, Y, and Z Coordinate Calculation

Number of frames: 2		Number of markers: 10	
7.1348953	50.8270798	52.6812515	
4.0118074	49.7802429	42.5428810	
6.6061921	53.5047340	31.6916409	
13.7037172	61.8890877	3.4096825	
11.2481747	83.8506622	-6.8301620	
-4.4081936	73.8573608	-2.3287313	
1.3992792	85.4378967	-8.2537441	
-26.0299950	55.7569504	33.3879662	
52.1080284	17.8120613	53.7419434	
61.8897438	15.6240826	3.9397044	
6.6324863	50.1592369	52.7665749	
3.9590020	49.6241035	42.4315453	
6.6526546	53.3926659	31.8468933	
14.4030781	62.1061668	2.9064591	
11.3370943	84.2221756	-5.9553838	
-4.0715818	74.1440277	-2.1017463	
1.9560380	86.0323105	-7.2709274	
-26.0426235	55.6070328	33.3775406	
52.2055206	17.7078915	53.7237244	
61.7921257	15.6955709	3.8837261	

Figure 3.17 File Format for a Typical *.tdc

For this *Start Up Information* option there is only one prompt which is to input the number of cameras that are being used. Currently the program allows the operator to choose from two or three cameras. The dialog box that appears for this option is shown in Figure 3.18. When two cameras are chosen the *Coordinate Calculation* option is configured for information from only two cameras. The program defaults to two cameras when this command is first executed.

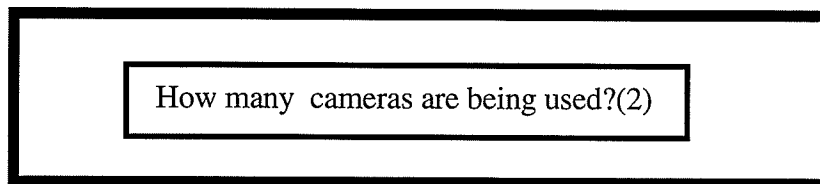


Figure 3.18 Start Up Information

File names of the calibration parameters (CPs) and the marker motion data are specified respectively in the *Calibration Input Files* and *Marker Data Files* options. The marker motion data files contain the two dimensional (U_i^k, V_i^k) camera view motion data.

The menus for specifying the calibration parameters and the marker motion data are shown in Figure 3.19 a and b respectively.

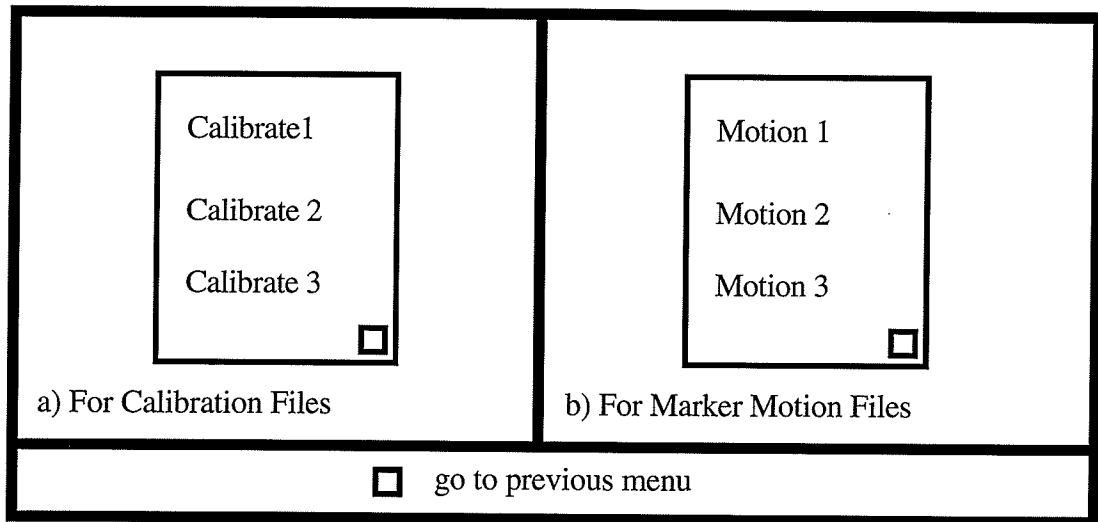


Figure 3.19 Menu for Calibration and Marker Motion Data Files

This *Output File* option allows the operator to specify the file that the calculated 3-D real world UL centroids are to be saved in. Usually the file is of the format *.tdc where tdc stands for "three dimensional calculation".

The *Process Coordinates* option allows the operator to calculate the 3-D real world UL centroids for the marker motion data. In sequence the calibration parameters are read into arrays; each set of 2-D camera view marker centroids is also read in. Then the three dimensional coordinate conversion is performed using the linear algebra discussed in Section 2.4. The information is saved to the specified output file (*.tdc) for later use. All the mathematical calculations are performed so that they are imperceptible to the operator.

The *Display Coordinates* option allows the operator to view the calculated coordinates. One frame of 3-D real world UL marker centroids are shown at a time. To see the next frame the space bar is pushed and this process is continued until all the marker coordinates are viewed. This option does not allow the operator to scroll backwards through the file.

3.7 Calculate Euler Angles

This section allows the operator to calculate the Euler angles for the shoulder, elbow, and wrist joints. The *Input File* option allows the operator to enter manually or by mouse the name of the file containing the calculated three dimensional data (*.tdc). The *Output Files* option allows the operator to specify the names of three files that will contain the shoulder (*.shd), elbow (*.elb), and wrist (*.wst) joint Euler angles. This option has a sub menu shown on the right in Figure 3.20 that specifies three options for entering the appropriate file names. Once the two previous options have been completed the *Process* option can be entered. This option reads in the three dimensional marker motion data

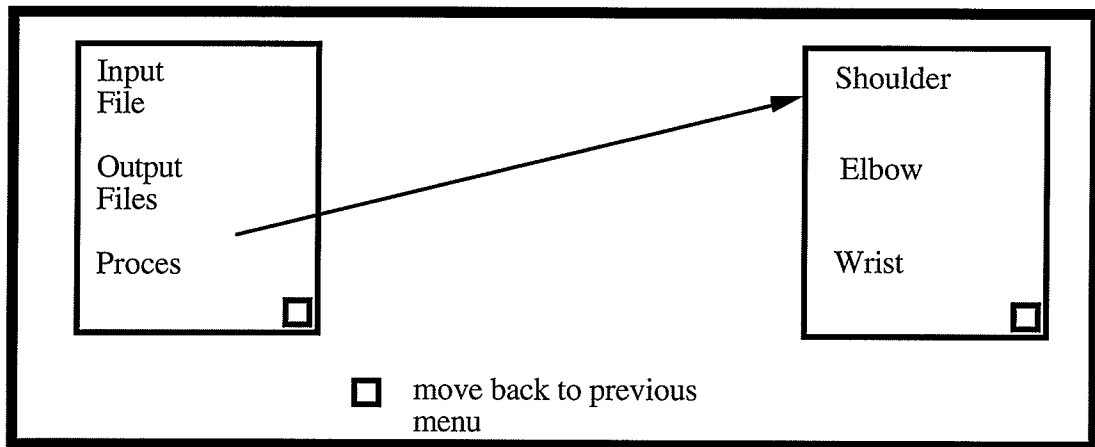


Figure 3.20 Main Euler Angle Calculation Menu

from the input file (*.tdc) and uses it to calculate the Euler angles which are then stored in the appropriate output files. A typical *.wst file is shown in Figure 3.21. The three columns respectively represent rotation about the z axis ϕ , rotation about the x^1 axis θ , and rotation about the y^2 axis ψ as defined in Section 3.5.

-10.74	5.97	0.52
-10.81	7.01	0.83
-10.96	8.35	0.90
-11.55	8.36	1.21
-11.55	8.35	1.97

**Figure 3.21 Euler Angle Data File Format
(* .wst)**

CHAPTER IV

Error Identification and its Progression Through UM²AS

This Chapter considers error present in the input parameters (U,V camera view control ball centroids, measured X, Y, and Z coordinates of the control ball centroids, and the U,V 2-D centroids of the upper limb) of the University of Manitoba Motion Analysis System (UM²AS) and how it affects the accuracy of the calculated three dimensional (3-D) centroids of the upper limb (UL) markers. An attempt is made to identify and quantify significant error sources in acquiring the input data. The effect of the errors in the U,V coordinates on the three dimensional coordinates is also quantified.

Observations made on the overall UM²AS system indicate that error occurs in such areas as the manual measurement coordinates, misalignment of the cameras, and in the method used to obtain the two dimensional (2-D) camera view (U,V) marker centroids. Realistically, manual measurements can be done with a metric measuring tape to an accuracy of plus or minus 1mm. If the cameras are not aligned properly, large errors could occur in the calculated 3-D real world UL centroids. These two sources of error were ruled against being the cause of a substantial effect on the 3-D centroids of the markers because they are controllable and/or minimal. Possible causes for the camera view centroid error are lens distortion, camera image quantization, and the markers being partially hidden from the view of the camera or distorted due to image noise. All three camera image errors cause the marker's shape to be distorted and the two dimensional camera position of its centroid to be improperly defined.

Before the sensitivity of UM²AS to camera view marker centroid error can be determined, the effects of the camera aspect ratio must be removed from the camera view marker centroids. The aspect ratio is a number that defines the ratio of the screen height to it's width. The image coming from the camera is rectangular in nature and the memory array in which the image is stored in is a square array. This causes the image to be either

compressed in the horizontal direction or stretched in the vertical direction. Section 4.1 quantifies the effect of the aspect ratio on the camera view marker centroids.

It is concluded that the error is concentrated in the camera view centroids of the markers, therefore their centroids are perturbed from the actual coordinates to simulate lens distortion, image quantization and image noise. The method for quantifying the error is to first perturb the camera view marker centroids of the control balls (CBs) and calculate the perturbation in the calibration parameters. The next step is to use the perturbed calibration parameters and the perturbation of the UL camera view centroids to calculate the perturbation of the 3-D real world marker centroids of the UL.

4.1 Determining the Aspect Ratio of the Cameras

An experiment was conducted to find the aspect ratio for camera 1. An apparatus termed "distortion jig" was constructed using the following materials:

wooden bar	-	length - 100 cm width - 3.1 cm
flat reflective markers	-	diameter - 3.8 cm quantity - 14
backing plate	-	diameter - 30 cm material - wood
anchor	-	metal

The apparatus was attached to the top of one of the tripods used in the lighting apparatus (Figure 4.1). The reflective markers were equally spaced at 7 cm intervals along the bar. Markers 7 and 8 were spaced a distance of 10 cm apart to allow for the mounting bolt that attached the bar to the light stand. There were holes in the backing plate placed at angular

increments of 36 degrees, which allowed the wooden bar to be bolted down and fixed at a defined angle.

The distortion jig was placed in front of the camera, within the viewing space. It was aligned perpendicular to the camera lens in a manner that allowed the bar with reflective markers to be completely seen at any orientation. The bar was rotated by known increments of 36 degrees from an angle of 0 degrees to 360 degrees. At each angular step the reflective markers 1 through 14 were digitized and the distance d_i in units (as labeled in Figure 4.1) of pixel length was obtained.

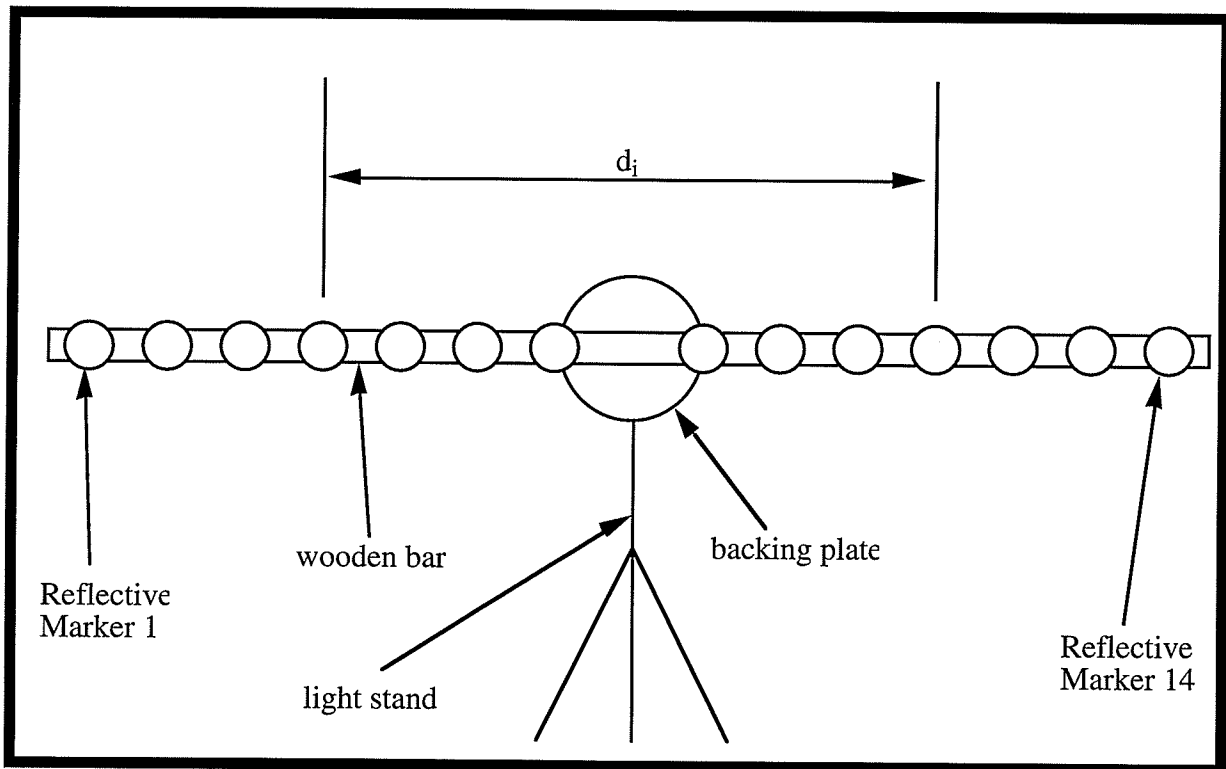


Figure 4.1 Rotating Apparatus for Checking Distortion

The distances between marker i and marker $15-i$ ($i \in (1,2,3,\dots,7)$) were calculated for each angular step using

$$d_i = \sqrt{(U_{(15-i)}^k - U_i^k)^2 + (V_{(15-i)}^k - V_i^k)^2} \quad (4.1)$$

The results of this experiment are shown in Figure 4.2. The graph illustrates that the distance between the digitized markers varied as the angle the bar made with the horizontal was changed. The distance d_i varied by as much as 71.77 pixel lengths.

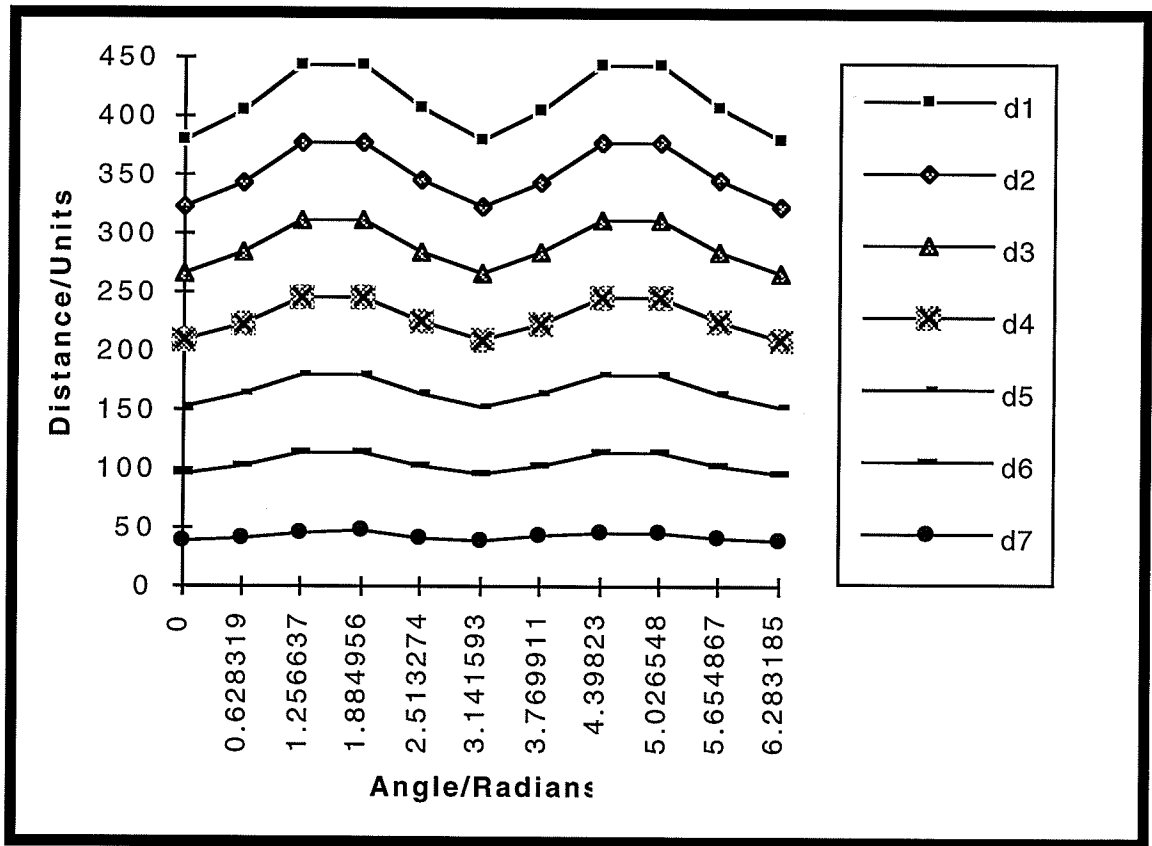


Figure 4.2 Distance Between Selected Marker Pairs

It is known that the real world distance between the marker pairs is constant therefore the camera view distance should also be constant. This has been shown to not be the case, therefore some type of distortion must be present. It has been hypothesized that the representations of the video image by the cameras and by the digitizing board are different, thus causing the distortion. The distortion is a stretching or shrinking of either the U or V component and therefore can be compensated for by applying a scaling factor to

either the components of the marker's camera view centroid. For the purpose of this investigation V was chosen. To solve this distortion problem, an aspect ratio correction (scaling factor) was applied to the V components of each marker as done in Equation 4.2 for markers 1 to 14.

$$\text{Correct } V_i^k = CF_{\text{avg}}^k V_i^k \quad (4.2)$$

At the point where the bar of the distortion jig is horizontal in the camera plane it was found that $V_{(15-i)}^k$ equals V_i^k . For this special case, the V components that possess all the error cancel out of Equation 4.1. Thus the true distance for d_i in terms of pixel lengths is given by

$$d_i^k = \left(U_{(15-i)}^k - U_i^k \right) \text{ when bar is horizontal} \quad \text{pixel lengths.} \quad (4.3)$$

The next step was to find the aspect ratio correction factor (CF_{avg}^k). This was done by realizing that a scaling factor can be applied to V_i^k that will satisfy

$$\left(CF_i^k = \frac{(d_i^k)^2 - (U_{(15-i)}^k - U_i^k)^2}{(V_{(15-i)}^k - V_i^k)^2} \right) \text{done for each angle increment} \quad (4.4)$$

Equation 4.4 generated seven absolute correction factors for each angle increment, therefore to find the average correction factor Equation 4.5 was used.

$$CF_{avg}^k = \frac{1}{n} \sum_{i=1}^n CF_i^k \quad (4.5)$$

The average correction factor that was calculated is 0.8407, which is approximately the aspect ratio of camera one which has an aspect ratio of 485(V)/570(H)= 0.8509. This aspect ratio meets and exceeds the RS-170 standard which states that a video system must have an aspect ratio of at least 330/525 = 0.629 [9,pp. 51]. Figure 4.3 shows the results of applying the aspect ratio correction; the maximum error now is approximately 0.5 pixel lengths.

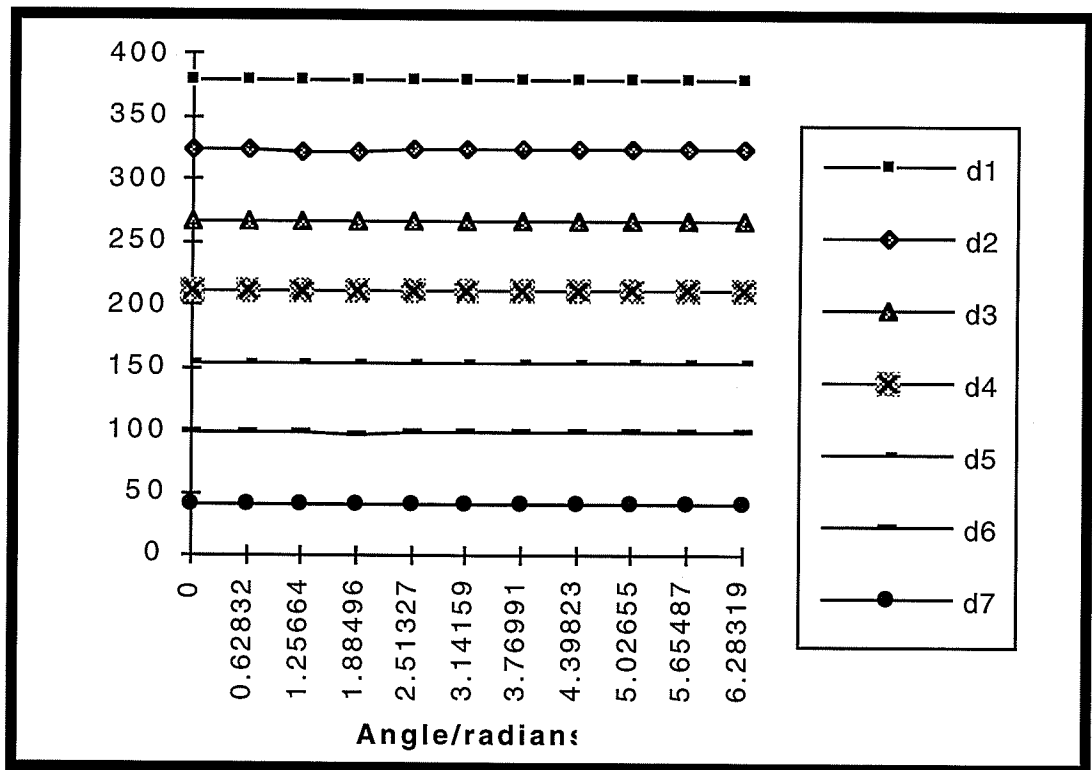


Figure 4.3 Corrected Distances between Selected Marker Pairs

4.2 Determining the Magnitude of Error in the Camera View Centroids

Now that the aspect ratio is accounted for, the error due to lens distortion, space quantization, and marker distortion can be quantified. The error due to lens distortion and space quantization are considered together in this analysis as camera error. To demonstrate that camera error does exist a simple experiment was performed. The distances between four markers were measured with a tape measure and were also found by calculating the 3-D real world marker centroids of the four markers with UM²AS. Table 4.1 summarizes the results of this experiment and verifies that the calculated centroids are different from the actual measured centroids, thus some camera error must be present.

Table 4.1

Marker Pair	Measured Distance (cm)	Calculated Distance(cm)	Relative Error (%)
4 - 1	30.5	30.86	-1.18
4 - 2	31.1	31.42	-1.07
4 - 3	30.2	30.55	-1.14
1 - 2	30.4	30.52	-0.39
1 - 3	30.5	30.65	-0.49
2 - 3	30.3	30.64	-1.11

Results of Relative Distance Error Test

Lens distortion combined with space quantization cause the markers to appear distorted and only approximately in the right location, therefore the centroid of the marker can not be calculated accurately. The magnitude of error can be determined by observing the remaining error after the aspect ratio correction has been performed. When determining the aspect ratio of the camera the markers used were not hidden, therefore the only remaining cause for error is due to lens distortion and space quantization. This error was experimentally found to be 0.5 pixel lengths in magnitude at maximum.

The second error source, marker distortion, is caused by the marker being partially hidden in the camera view by objects in the experiment, by the upper limb (UL), or by

being engulfed by surrounding noise caused by white light reflecting off apparatus or the subject in the viewing area. A good estimate of the maximum possible error contributed by marker distortion is to determine the maximum diameter of the marker in the camera view. This occurs when the marker is closest to the camera without leaving the viewing space. The diameter was found to be 25 pixel lengths and therefore if the marker approaches complete coverage then the centre will be perturbed by half the diameter or 12.5 pixel lengths.

The maximum magnitude of error in the UL camera view centroids is calculated by summing both the maximum error magnitudes (camera distortion and marker distortion) to yield 13 pixel lengths. The errors are algebraically summed because these errors only represent a distance from the actual point not a direction therefore the total error represents a radius of 13 pixel lengths with the origin located at the location of the actual point.

4.3 Sensitivity Analysis

The previous section showed that the 2-D camera view centroids are not error free. This is not a problem as long as the error is not magnified and compounded as it propagates through UM²AS. The goal of this section is to quantify error in the calculated 3-D real world centroids caused by error in the camera view centroids of the calibration parameters and the UL markers.

An analytical method for quantifying error is based on perturbing A and b in $Ax=b$. This method is used because the equation used to find the calibration parameters for example takes on this form as shown by

$$\mathbf{A} \begin{bmatrix} L_1^k \\ L_2^k \\ \vdots \\ L_{10}^k \\ L_{11}^k \end{bmatrix} = \mathbf{b}. \quad (4.6)$$

where

$$\mathbf{A} = \begin{bmatrix} X_1^{CB} & Y_1^{CB} & Z_1^{CB} & 1 & 0 & 0 & 0 & 0 & -U_1^k X_1^{CB} & -U_1^k Y_1^{CB} & -U_1^k Z_1^{CB} \\ 0 & 0 & 0 & 0 & X_1^{CB} & Y_1^{CB} & Z_1^{CB} & 1 & -V_1^k X_1^{CB} & -V_1^k Y_1^{CB} & -V_1^k Z_1^{CB} \\ X_2^{CB} & Y_2^{CB} & Z_2^{CB} & 1 & 0 & 0 & 0 & 0 & -U_2^k X_2^{CB} & -U_2^k Y_2^{CB} & -U_2^k Z_2^{CB} \\ 0 & 0 & 0 & 0 & X_2^{CB} & Y_2^{CB} & Z_2^{CB} & 1 & -V_2^k X_2^{CB} & -V_2^k Y_2^{CB} & -V_2^k Z_2^{CB} \\ \vdots & \vdots \\ X_8^{CB} & Y_8^{CB} & Z_8^{CB} & 1 & 0 & 0 & 0 & 0 & -U_8^k X_8^{CB} & -U_8^k Y_8^{CB} & -U_8^k Z_8^{CB} \\ 0 & 0 & 0 & 0 & X_8^{CB} & Y_8^{CB} & Z_8^{CB} & 1 & -V_8^k X_8^{CB} & -V_8^k Y_8^{CB} & -V_8^k Z_8^{CB} \end{bmatrix}$$

$$\mathbf{b} = \begin{bmatrix} U_1^k \\ V_1^k \\ U_2^k \\ V_2^k \\ \vdots \\ U_8^k \\ V_8^k \end{bmatrix}$$

$(X_i^{CB}, Y_i^{CB}, Z_i^{CB})$ - measured control ball (CB) centroid \mathbf{i}

(U_i^k, V_i^k) - 2-D camera view CB centroid \mathbf{i} for camera \mathbf{k}

One way to quantify the perturbation of the calibration parameters is to use the analytical expression

$$\frac{\|\delta L\|}{\|L\|} \leq \frac{\|A^{-1}\|}{1 - \|A^{-1}\| \|\delta A\|} \left(\frac{\|\delta b\|}{\|L\|} + \|\delta A\| \right), \quad (4.7)$$

which is found in [14, pp. 121]. Equation 4.7 has a condition under which it can be used.

This condition is

$$\|A^{-1}\| \|\delta A\| < 1. \quad (4.8)$$

Unfortunately this condition was not met by the perturbed matrices.

There are possibly other methods of quantifying the perturbation, but none were located in the literature. The method chosen to quantify error was to perturb the 2-D camera view centroids of the control balls and the upper limb (UL) markers by a defined amount from their actual location (Figure 4.4). Section 4.3.1 demonstrates how the error in the 2-D camera view centroids propagates through to the calibration parameters and Section 4.3.2 shows how error propagates from the 2-D camera view marker centroids of the UL to the calculated 3-D real world centroids of the UL.

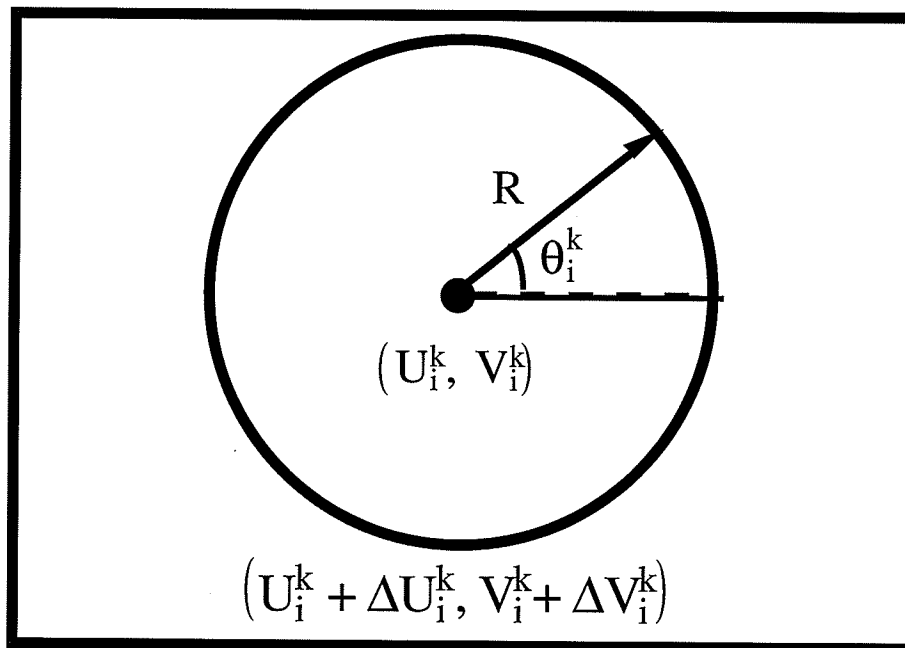


Figure 4.4 Polar Coordinate Representation of

4.3.1 Calibration Parameter (CP) Sensitivity

The main assumption made was that the error is in the 2-D camera view CB centroids as opposed to the tape measured CB centroids. Therefore the digitized 2-D CB camera view centroids can be expressed as the actual component plus some variation delta $(U_i^k + \Delta U_i^k, V_i^k + \Delta V_i^k)$. The deltas or perturbation amounts were obtained by using Equation 4.9 and Equation 4.10. These equations represent a polar coordinate conversion from Cartesian coordinates. This was done because the error could be at any position about the actual centroid of the marker by a certain distance which in this case is called R. Therefore it makes more sense to carry out the perturbation with a polar coordinate system rather than Cartesian.

$$\Delta U_i^k = R \cos(\theta_i^k) \quad (4.9)$$

$$\Delta V_i^k = R \sin(\theta_i^k) \quad (4.10)$$

where i is the marker index (varies from 1 to 8), k is the camera index (varies from 1 to 3), R is the distance from the i^{th} marker centroid in the camera view k (0.5 pixels), and θ_i^k is the rotation (in radians) around the i^{th} marker centroid from camera k .

The actual L parameters are determined by Equation 2.1. To find the calibration parameters when the 2-D CB camera view centroids are perturbed, the addition of the deltas (defined in Equation 4.9 and Equation 4.10) to all the 2-D CB camera view centroids (U_i^k, V_i^k) is required.

$$\%error = 100 \sqrt{\frac{\sum_{i=1}^{11} ((L_i^k)_{\text{perturbed}} - (L_i^k)_{\text{actual}})^2}{\sum_{i=1}^{11} ((L_i^k)_{\text{actual}})^2}} \quad (4.11)$$

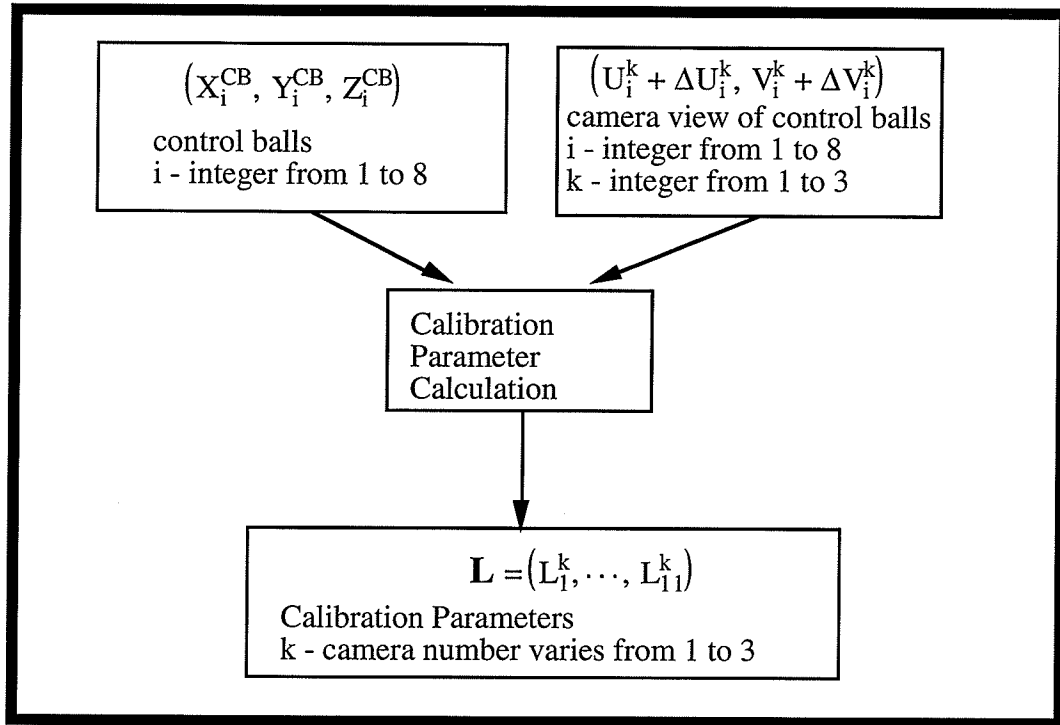


Figure 4.5 Flow Chart of Error flow from the Control Ball Camera View Coordinates to the Calibration Parameters

By choosing different values for R ($R = 2, R = 1.5, R = 1.0,$ or $R = 0.5$) and randomly varying θ_i^k (θ_i^k - varied randomly between 0 and 180 degrees), it was concluded that as R increases so does the percent error given by Equation 4.11. From Section 4.2 it was found that the maximum error magnitude was 0.5 pixel lengths. Therefore the largest R will ever be is 0.5 pixel lengths, when calculating the calibration parameters.

To acquire a good indication of the maximum error, θ_i^k was randomly varied while R was set to 0.5 pixel lengths (the upper bound). It was found that the maximum perturbation

error of the calibration parameters given in these random samples (1 million samples) was 0.70%. At this error the perturbed calibration parameter values are shown in Table 4.2. The third column shows the error between the actual and perturbed calibration parameter value. The calibration parameter error is small accept for three cases. These cases have actual and perturbed calibration parameter that are small and therefore contribute very little to the overall effect of the calibration parameters. Similar results were obtained for camera two and three as well.

Table 4.2

Actual L	Perturbed L	%Error
-0.9359012	-0.9164725	2.08
4.0529704	4.1039071	1.26
0.0655944	0.0780605	19.0
94.7372513	93.3254852	1.49
-0.8824302	-0.8767406	0.64
0.0630595	0.0625963	0.73
-4.8949742	-4.9290571	0.70
410.1895447	412.7666931	0.63
-0.0037763	-0.0036892	2.31
-0.0001727	-0.0001282	25.77
-0.0001233	-0.0000876	28.95

Relative Error of each L Parameter

4.3.2 Proposed Real World Coordinate Sensitivity Method

Sensitivity of the calculated real world coordinates is approached in the following manner (Figure 4.6). The three sets of 2-D upper limb camera view marker centroids vary according to $(U_i^1 + \Delta U_i^1, V_i^1 + \Delta V_i^1)$, $(U_i^2 + \Delta U_i^2, V_i^2 + \Delta V_i^2)$, and $(U_i^3 + \Delta U_i^3, V_i^3 + \Delta V_i^3)$.

The perturbed real world UL centroids are given by Equation 2.5 except that $(U_i^1 + \Delta U_i^1, V_i^1 + \Delta V_i^1)$, $(U_i^2 + \Delta U_i^2, V_i^2 + \Delta V_i^2)$, $(U_i^3 + \Delta U_i^3, V_i^3 + \Delta V_i^3)$ and replace the 2-D UL camera view centroids for camera one, two, and three. To calculate the error distance between the actual real world and the perturbed real world UL centroid use Equation 4.12.

$$\%error = 100 \sqrt{\frac{((X_i^{avg})_p - (X_i^{avg})_a)^2 + ((Y_i^{avg})_p - (Y_i^{avg})_a)^2 + ((Z_i^{avg})_p - (Z_i^{avg})_a)^2}{((X_i^{avg})_a)^2 + ((Y_i^{avg})_a)^2 + ((Z_i^{avg})_a)^2}} \quad (4.12)$$

where

p - perturbed
a - actual

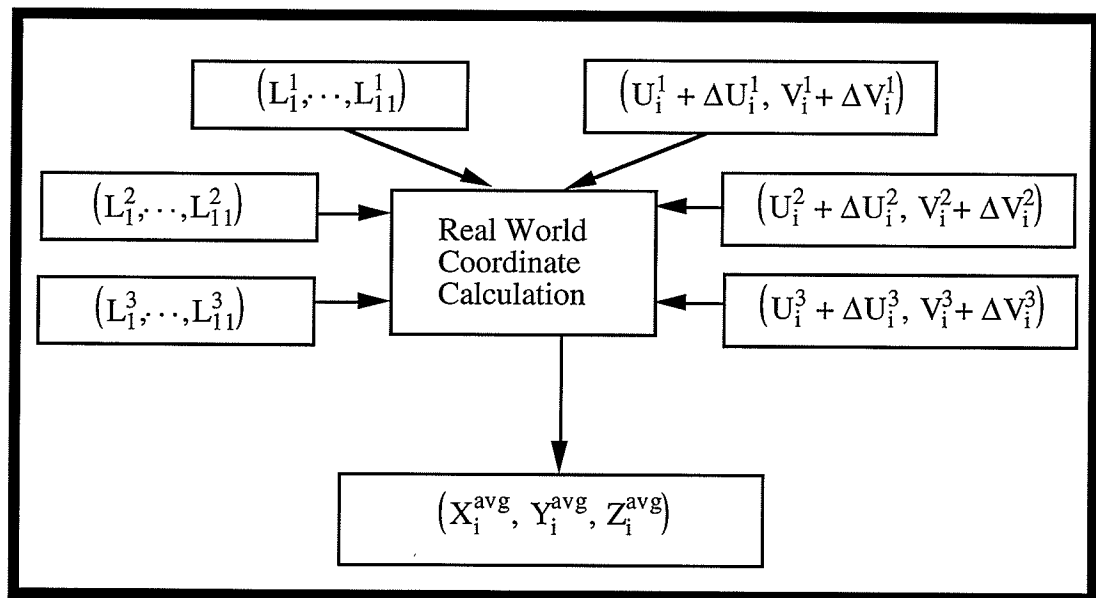


Figure 4.6 Flow Chart of Error Propagation from the Marker Camera View Coordinates to the Calculated Real World Coordinates

To ascertain at which location along the radius R the maximum error was likely to occur theta was first randomly varied and then various values of R were chosen (R = 13, 12.9, 7, 4, 3) which were then applied to the perturbation equations given in (4.12) and (4.13). Theta was varied a million times and the maximum error was found to always occur when R = 13 pixel lengths. It has been found that the maximum error given by equation 4.15 was 4.56% or a Euclidean distance of 3.28 cm away from the actual location of the marker. The final step was to repeat the process with the perturbed calibration parameters.

It was then found that the error went up to 4.62% or a Euclidean distance of 3.32 cm away from the actual marker location.

CHAPTER V

CONCLUSION

The goals of the present changes to the University of Manitoba Motion Analysis System (UM²AS) were to: 1) reduce the loss of upper limb (UL) marker information, 2) improve the software to make it more operator friendly and more acceptable in a clinical environment, and 3) isolate UM²AS input data error and develop a method of checking the sensitivity of UM²AS to that error.

Initially UM²AS was a two camera system and occasionally UL motion markers would disappear from one or both of the camera views (one more frequently than both). If this occurred the three-dimensional (3-D) calculated real world centroids of the UL markers could not be found. The addition of a third camera largely eliminated this problem because it allowed UM²AS to have more input data from different vantage points.

To improve the software of UM²AS an integrated environment was created that is a largely mouse driven, pop up window system. This style of program was found easy to use by operators that applied it to related tasks throughout its development. The reasons given by operators are that little knowledge of computers is needed, there are few key commands to remember, it is easy to make changes to any previous entries made, and the software is esthetically pleasing.

Error in the calculated 3-D real world centroids was found to stem from the 2-D calculated camera view centroids. It was found that after an aspect ratio correction was performed, the error was typically only 0.5 pixel lengths in magnitude for markers that are always in full view (calibration balls) and about 13 pixel lengths for markers that are hidden or engulfed in noise (upper limb markers). The sensitivity analysis was applied to UM²AS and it was evident that the system is most sensitive to error in the 2-D UL camera view centroids.

The following recommendations are presented for further development of the UM²AS system.

1) Replace the Beta players with VHS VCR's. VHS is the preferred format and there are VHS players with hardware that allows direct link with the computer. The advantage to this is that the computer, rather than the operator, will control the frame-by-frame advance of the tape and all the VCR commands can be put on a menu which would appear on the computer screen. This will help reduce human error and will speed up the data acquisition process.

2) As the system grows it will use more than 640 kilobytes of working memory (executable file currently consumes 223 kilobytes of memory). DOS based programs are limited to 640 kilobytes. An alternative is to consider programming the software for the Windows operating system. Preliminary work has been done on this task and the reported advantages of a Windows based system are: a) the Windows operating system allows the program to use all available RAM, b) better video resolution is available therefore a more detailed simulation of the upper limb can be created, and c) it is much easier to create a integrated environment under Windows that will be more commercially acceptable. More working RAM and C++ classes (found with the C++ compiler) will make operations like curve smoothing and graphing the Euler angles easy to program (Euler angles will no longer have to be imported into a spread sheet type of program for curve smoothing and graphing). This will enhance the overall look of the software and will also speed up the data analysis process. Creating an integrated environment in Windows is much easier than in DOS because most of the pop up windows, action buttons, and printer interfacing is already available with the currently used C++ compiler. On-line key word search help or operator manual could also be easily created (one day learning curve).

3) A program that presents an animated simulation of the upper limb (UL) motion should be created. This type of display will give the operator a tool to visualize the UL from a variety of different vantage points thereby offering new information about the UL motion. This software should be created as a Windows application, because Windows has a suitable graphical interface.

4) The currently used image processing board has no software support for a Windows application type of system. To enter the Windows environment an image processing board with Windows support as well as DOS support should be purchased.

REFERENCES

- [1] American Academy of Orthopaedic Surgeons, "Joint Motion: Method of Measuring and Recording", Chicago, American Academy of Orthopaedic Surgeons, 1965.
- [2] Anderson J.E., "Grant's Atlas of Anatomy: Eighth Edition", Williams & Wilkins, 1983.
- [3] Antonsson E. K., Mann R. W., "Automatic 6-D.O.F. Kinematic Trajectory Acquisition and Analysis", Journal of Dynamic Systems, Measurement, and Control, Vol. 111, 31 - 39, March 1989.
- [4] Cooper J. E., Quanbury A. O., Safaee-Rad R., Shwedyk E., "Normal Functional Range of Motion of Upper Limb Joints During Performance of Three Feeding Activities", Arch Phys Med Rehabil, Vol 71, 505 - 509, June 1990.
- [5] Dempster, S. T., "The Anthropometry of Body Motion", Annals New York Academy of Sciences, Vol. 63: 559-585, 1955.
- [6] Frankel V. H. , Nordin M., "Basic Biomechanics of the Skeletal System", Philadelphia, Lea & Febiger, 1980.
- [7] Gonzalez R. C. , Wintz P., "Digital Image Processing", Don Mills, Ontario, Addison-Wesley Publishing Company, Inc. ,1987.

- [8] Gowitzke B. A. , Milner M. , "Scientific Bases of Human Movement: Third Edition", Baltimore, Williams & Wilkins, 1988.
- [9] Lindley C., "Practical Image Processing In C", New York, John Wiley & Sons, Inc., 1991.
- [10] Macleod K. A. , "A Marker Detection Algorithm For The Study Of Functional Human Arm Movements", Fourth Year Thesis, Dept. of Electrical & Computer Eng., University of Manitoba, 1990.
- [11] Quanbury A. O. , Safae-Rad R. , Shweddyk E., "Three-dimensional measurement system for functional arm motion study", Med. & Biol. Eng. & Comput., Vol. 28, 569-573, 1990.
- [12] Safae-Rad, R., "Functional Human Arm Motion Study With A New 3-D Measurement System (VCR-PIPEZ-PC)", M.Sc. Thesis, Dept. of Electrical and Computer Eng., University of Manitoba, 1987.
- [13] Usmani, R. A., "Applied Linear Algebra", New York and Basel, Marcel Dekker, INC., 1987.
- [14] Usmani, R. A., "Numerical Analysis for Beginners", Canada, D.W. Friesen & Sons, 1991.
- [15] Winter, D., "Biomechanics of Human Movement", New York, John Wiley & Sons, Inc., 1979.

[16]

Youm, Y., Yoon, Y. S., "Analytical Development in Investigation of Wrist Kinematics", J. Biomechanics, Vol. 12: 613-621, 1979.

APPENDIX A

Derivation Of Euler Angular Formulas (Angular Rotations)

The following is a derivation of the Euler angles for the shoulder, elbow, and wrist joints. It starts with the fact that any rotation will be defined as a rotation about an axis. The Euler angles $(\phi_i, \theta_i, \psi_i)$ are angular rotations about the real world coordinate system (X, Y, Z) that cause it to be rotated to the position of the i^{th} auxiliary coordinate system. The Euler angles are applied in the following order. ϕ_i is the rotation about the Z axis of the axis system (X, Y, Z) . This rotates the real world coordinate system to a new position termed (x_i^1, y_i^1, z_i^1) given by

$$\begin{bmatrix} x_i^1 \\ y_i^1 \\ z_i^1 \end{bmatrix} = \begin{bmatrix} \cos\phi_i & \sin\phi_i & 0 \\ -\sin\phi_i & \cos\phi_i & 0 \\ 0 & 0 & 1 \end{bmatrix} \begin{bmatrix} X \\ Y \\ Z \end{bmatrix}. \quad (\text{A.1})$$

The next rotation applied is the one about the x_i^1 axis termed θ_i . This rotation moves the coordinate system to a new position termed (x_i^2, y_i^2, z_i^2) given by

$$\begin{bmatrix} x_i^2 \\ y_i^2 \\ z_i^2 \end{bmatrix} = \begin{bmatrix} 1 & 0 & 0 \\ 0 & \cos\theta_i & \sin\theta_i \\ 0 & -\sin\theta_i & \cos\theta_i \end{bmatrix} \begin{bmatrix} x_i^1 \\ y_i^1 \\ z_i^1 \end{bmatrix}. \quad (\text{A.2})$$

The last rotation ψ_i rotates the axis system about the y_i^2 axis to become the desired auxiliary axis system (x_i, y_i, z_i) .

$$\begin{bmatrix} x_i \\ y_i \\ z_i \end{bmatrix} = \begin{bmatrix} \cos\psi_i & 0 & -\sin\psi_i \\ 0 & 1 & 0 \\ \sin\psi_i & 0 & \cos\psi_i \end{bmatrix} \begin{bmatrix} x_i^2 \\ y_i^2 \\ z_i^2 \end{bmatrix} \quad (\text{A.3})$$

When the rotations are combined in the proper order, transformation Equation A.4 is

obtained which relates the i^{th} auxiliary system (x_i, y_i, z_i) to the real world axis system (X, Y, Z) .

$$\begin{bmatrix} x_i \\ y_i \\ z_i \end{bmatrix} = \mathbf{T}_i \begin{bmatrix} X \\ Y \\ Z \end{bmatrix} \quad (\text{A.4})$$

Where

$$\mathbf{E}_i = \begin{bmatrix} \cos\phi_i \cos\psi_i - \sin\phi_i \sin\theta_i \sin\psi_i & \sin\phi_i \cos\psi_i + \cos\phi_i \sin\theta_i \sin\psi_i & -\cos\theta_i \sin\psi_i \\ -\sin\phi_i \cos\theta_i & \cos\phi_i \cos\theta_i & \sin\theta_i \\ \cos\phi_i \sin\psi_i + \sin\phi_i \sin\theta_i \cos\psi_i & \sin\phi_i \sin\psi_i - \cos\phi_i \sin\theta_i \cos\psi_i & \cos\theta_i \cos\psi_i \end{bmatrix}$$

Let $(\hat{i}_i, \hat{j}_i, \hat{k}_i)$ be the unit vectors of the orthogonal auxiliary axis system (x_i, y_i, z_i) axis and $(\hat{I}, \hat{J}, \hat{K})$ be the unit vectors of real world axis system (X, Y, Z) , then equation A.4 can be also written as Equation A.5.

$$\begin{bmatrix} x_i \\ y_i \\ z_i \end{bmatrix} = \mathbf{A}_i \begin{bmatrix} X \\ Y \\ Z \end{bmatrix} \quad (\text{A.5})$$

Where

$$\mathbf{A}_i = \begin{bmatrix} \hat{i}_i \hat{I} & \hat{i}_i \hat{J} & \hat{i}_i \hat{K} \\ \hat{j}_i \hat{I} & \hat{j}_i \hat{J} & \hat{j}_i \hat{K} \\ \hat{k}_i \hat{I} & \hat{k}_i \hat{J} & \hat{k}_i \hat{K} \end{bmatrix}$$

Thus matrix A must equal matrix E and therefore $(\phi_i, \theta_i, \psi_i)$ can be calculated using Equations A.6, A.7, and A.8.

$$\sin\theta_i = \hat{j}_i \cdot \hat{k}_i \rightarrow \theta_i = \sin^{-1} (\hat{j}_i \cdot \hat{k}_i) \quad (\text{A.6})$$

$$\cos\phi_i \cos\theta_i = \hat{j}_i \cdot \hat{J} \rightarrow \phi_i = \cos^{-1} \left(\frac{\hat{j}_i \cdot \hat{J}}{\cos\theta_i} \right) \quad (\text{A.7})$$

$$\cos\theta_i \cos\psi_i = \hat{k}_i \cdot \hat{K} \rightarrow \psi_i = \cos^{-1} \left(\frac{\hat{k}_i \cdot \hat{K}}{\cos\theta_i} \right) \quad (\text{A.8})$$

The above shows how to find the Euler angles for the i^{th} arbitrary auxiliary system. For the purpose of the upper limb model three auxiliary systems that model the shoulder joint, elbow joints, and wrist joint must be found. This is done by first modelling the upper limb as an eight degree of freedom (DOF) system consisting of:

- 3 DOF - at the shoulder joint
- 2 DOF - at the elbow region joints
- 3 DOF - at the wrist joint

To achieve this, seven reflective markers as in Figure a.1, are used to calculate the eight rotations. To calculate these eight angular rotations relative to the upper limb, four auxiliary axis systems must be defined on the upper limb. These auxiliary systems define the regions: a) shoulder, b) arm, c) forearm, and d) hand. This is done in a manner that is illustrated in Figure A.1.

Shoulder

$$\vec{y}_0 = \vec{21} \quad (\text{A.9})$$

$$\vec{x}_0 = \vec{21} \times \vec{23} \quad (\text{A.10})$$

$$\vec{z}_0 = \vec{x}_0 \times \vec{y}_0 \quad (\text{A.11})$$

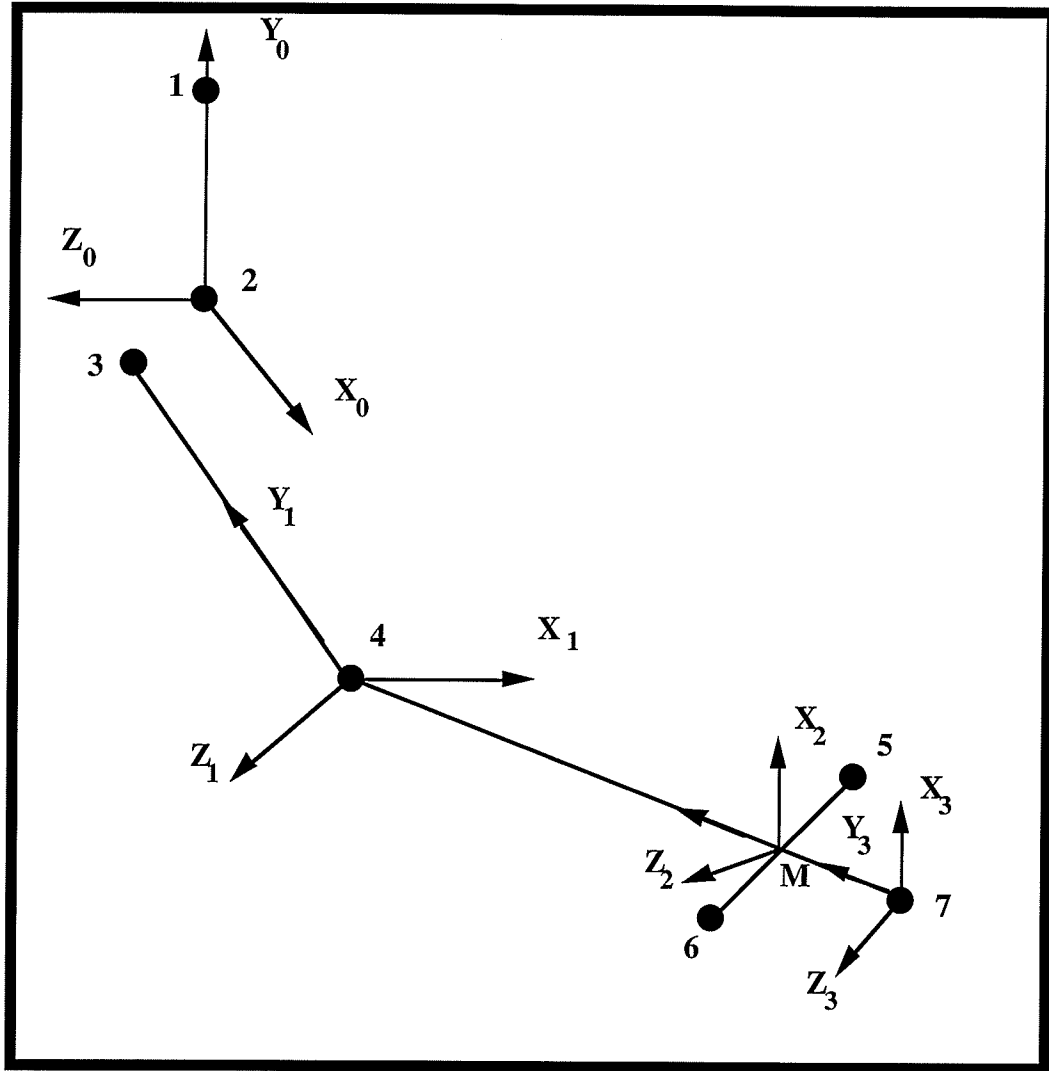


Figure A.1 Stick Diagram and Vector Directions for the Upper Limb Model

Arm

$$\vec{y}_1 = \vec{43} \quad (\text{A.12})$$

$$\vec{z}_1 = \vec{4M} \times \vec{43} \quad (\text{A.13})$$

$$\vec{x}_1 = \vec{y}_1 \times \vec{z}_1 \quad (\text{A.14})$$

Forearm

$$\vec{y}_2 = \vec{M4} \quad (\text{A.15})$$

$$\vec{x}_2 = \vec{46} \times \vec{45} \quad (\text{A.16})$$

$$\vec{z}_2 = \vec{x}_2 \times \vec{y}_2 \quad (\text{A.17})$$

Hand

$$\vec{y}_3 = \vec{7M} \quad (\text{A.18})$$

$$\vec{x}_3 = \vec{75} \times \vec{76} \quad (\text{A.19})$$

$$\vec{z}_3 = \vec{x}_3 \times \vec{y}_3 \quad (\text{A.20})$$

The rotations of the four regions of the upper limb referred to the real world coordinate system are defined as follows

Shoulder

$$E_0 = A_0 E \quad (\text{A.21})$$

Arm

$$E_1 = A_1 E \quad (\text{A.22})$$

Forearm

$$E_2 = A_2 E \quad (\text{A.23})$$

Hand

$$E_3 = A_3 E \quad (\text{A.24})$$

To define the joint rotations, they must be obtained with reference to the upper limb and not the real world coordinate system. These three rotations are defined in the following manner:

Shoulder joint

$$E_1 = A_1(A_0)^{-1}E_0 \rightarrow E_1 = R_1E_0 \quad (\text{A.25})$$

Elbow region joints

$$E_2 = A_2(A_1)^{-1}E_1 \rightarrow E_2 = R_2E_1 \quad (\text{A.26})$$

Wrist joint

$$E_3 = A_3(A_2)^{-1}E_2 \rightarrow E_3 = R_3E_2 \quad (\text{A.27})$$

where

$$E \quad - \quad [\hat{I} \quad \hat{J} \quad \hat{K}]$$

- matrix representation of the unit vectors for real world coordinate axis system

E_i - $\begin{bmatrix} \hat{i}_i & \hat{j}_i & \hat{k}_i \end{bmatrix}$
 - matrix representation of the unit vectors for the i^{th} body axis system

A_i - $\begin{bmatrix} \hat{i}_i \hat{I} & \hat{i}_i \hat{J} & \hat{i}_i \hat{K} \\ \hat{j}_i \hat{I} & \hat{j}_i \hat{J} & \hat{j}_i \hat{K} \\ \hat{k}_i \hat{I} & \hat{k}_i \hat{J} & \hat{k}_i \hat{K} \end{bmatrix}$
 - transformation matrix from the real world coordinate system to the auxiliary system

R_i - relative transformation matrix

The euler angles for each joint can be calculated by computing the relative transformation matrices. It is known that the matrix R_i is a 3x3 matrix therefore it can be defined by equation A.28.

$$R_i = \begin{bmatrix} r_{11}^i & r_{12}^i & r_{13}^i \\ r_{21}^i & r_{22}^i & r_{23}^i \\ r_{31}^i & r_{32}^i & r_{33}^i \end{bmatrix} \quad (\text{A.28})$$

Defining R_i in this manner yields the following equations for the rotation angles for the three joint regions.

Shoulder joint

$$\theta_1 = \sin^{-1} (r_{23}^1) \quad (\text{A.29})$$

$$\phi_1 = \cos^{-1} \left(\frac{r_{22}^1}{\cos \theta_1} \right) \quad (\text{A.30})$$

$$\psi_1 = \cos^{-1} \left(\frac{r_{33}^1}{\cos\theta_1} \right) \quad (\text{A.31})$$

Elbow region joints

$$\theta_2 = \sin^{-1} (r_{23}^2) \quad (\text{A.32})$$

$$\psi_2 = \cos^{-1} \left(\frac{r_{33}^2}{\cos\theta_2} \right) \quad (\text{A.33})$$

Wrist joint

$$\theta_3 = \sin^{-1} (r_{23}^3) \quad (\text{A.34})$$

$$\phi_3 = \cos^{-1} \left(\frac{r_{22}^3}{\cos\theta_3} \right) \quad (\text{A.35})$$

$$\psi_3 = \cos^{-1} \left(\frac{r_{33}^3}{\cos\theta_3} \right) \quad (\text{A.36})$$

APPENDIX B

Derivation of Calibration Parameter and Real World Coordinate Calculation Formulas

The assumption made in the UM²AS is that the relationship between the 3-D real world marker centroids (X_i, Y_i, Z_i) and the 2-D camera view marker centroids (U_i^k, V_i^k) is a linear perspective transformation. Equation B.1 performs this type of transformation.

$$\begin{bmatrix} U_i^k & V_i^k & 1 \end{bmatrix} = \begin{bmatrix} X_i & Y_i & Z_i & 1 \end{bmatrix} \begin{bmatrix} L_1^k & L_2^k & L_3^k & L_4^k \\ L_5^k & L_6^k & L_7^k & L_8^k \\ L_9^k & L_{10}^k & L_{11}^k & L_{12}^k \end{bmatrix}^T \quad (\text{B.1})$$

Where i is the marker number index, k is the camera number index, (X_i, Y_i, Z_i) is the i^{th} real world marker center, (U_i^k, V_i^k) is the i^{th} marker center from the camera view k , and (L_1^k, \dots, L_{12}^k) are the calibration parameters for camera k .

To calibrate the motion analysis system the parameters L_1^k through L_{12}^k must be found. This is achieved by expanding Equation B.1 into Equation B.2 and Equation B.3.

$$U_i^k = \frac{L_1^k X_i + L_2^k Y_i + L_3^k Z_i + L_4^k}{L_9^k X_i + L_{10}^k Y_i + L_{11}^k Z_i + L_{12}^k} \quad (\text{B.2})$$

$$V_i^k = \frac{L_5^k X_i + L_6^k Y_i + L_7^k Z_i + L_8^k}{L_9^k X_i + L_{10}^k Y_i + L_{11}^k Z_i + L_{12}^k} \quad (\text{B.3})$$

To reduce the number of parameters, Equation B.2 and Equation B.3 are scaled by dividing through by L_{12}^k which has the equivalent effect of setting L_{12}^k equal to one. This is done in Equation B.4 and Equation B.5.

$$U_i^k = \frac{L_1^k X_i + L_2^k Y_i + L_3^k Z_i + L_4^k}{L_9^k X_i + L_{10}^k Y_i + L_{11}^k Z_i + 1} \quad (\text{B.4})$$

$$V_i^k = \frac{L_5^k X_i + L_6^k Y_i + L_7^k Z_i + L_8^k}{L_9^k X_i + L_{10}^k Y_i + L_{11}^k Z_i + 1} \quad (\text{B.5})$$

Now it is possible to write two linear equations for each calibration view centroid (U_i^k, V_i^k) as shown by Equation B.6 and Equation B.7.

$$V_i^k = L_5^k X_i + L_6^k Y_i + L_7^k Z_i + L_8^k - V_i^k L_9^k X_i - V_i^k L_{10}^k Y_i - V_i^k L_{11}^k Z_i \quad (\text{B.6})$$

$$U_i^k = L_1^k X_i + L_2^k Y_i + L_3^k Z_i + L_4^k - U_i^k L_9^k X_i - U_i^k L_{10}^k Y_i - U_i^k L_{11}^k Z_i \quad (\text{B.7})$$

Equations B.6 and Equation B.7 are the basis for deriving the calibration parameters (CPs) and for calculating the 3-D real world marker centroids.

There are 11 CPs thus 11 independent equations are needed to solve for them. To achieve this the information needed is the 3-D real world marker centroid values $(X_i^{CB}, Y_i^{CB}, Z_i^{CB})$ and the 2-D camera view marker coordinates (U_i^k, V_i^k) of at least six markers or control balls (CBs). For the purpose of this project eight known control balls were used. Eight sets of the Equations B.6 and Equation B.7 are put into a matrix to yield equation B.8.

$$\begin{bmatrix} L_1^k & L_2^k & \dots & L_{10}^k & L_{11}^k \end{bmatrix}^T = (A^T A)^{-1} A^T \begin{bmatrix} U_1^k & V_1^k & U_2^k & V_2^k & \dots & U_8^k & V_8^k \end{bmatrix}^T \quad (\text{B.8})$$

Where

$$(A^T A)^{-1} A^T \quad - \quad \text{pseudo inverse}$$

$$\mathbf{A} = \begin{bmatrix} X_1^{CB} & Y_1^{CB} & Z_1^{CB} & 1 & 0 & 0 & 0 & 0 & -U_1^k X_1^{CB} - U_1^k Y_1^{CB} - U_1^k Z_1^{CB} \\ 0 & 0 & 0 & 0 & X_1^{CB} & Y_1^{CB} & Z_1^{CB} & 1 & -V_1^k X_1^{CB} - V_1^k Y_1^{CB} - V_1^k Z_1^{CB} \\ X_2^{CB} & Y_2^{CB} & Z_2^{CB} & 1 & 0 & 0 & 0 & 0 & -U_2^k X_2^{CB} - U_2^k Y_2^{CB} - U_2^k Z_2^{CB} \\ 0 & 0 & 0 & 0 & X_2^{CB} & Y_2^{CB} & Z_2^{CB} & 1 & -V_2^k X_2^{CB} - V_2^k Y_2^{CB} - V_2^k Z_2^{CB} \\ \vdots & \vdots \\ X_8^{CB} & Y_8^{CB} & Z_8^{CB} & 1 & 0 & 0 & 0 & 0 & -U_8^k X_8^{CB} - U_8^k Y_8^{CB} - U_8^k Z_8^{CB} \\ 0 & 0 & 0 & 0 & X_8^{CB} & Y_8^{CB} & Z_8^{CB} & 1 & -V_8^k X_8^{CB} - V_8^k Y_8^{CB} - V_8^k Z_8^{CB} \end{bmatrix}$$

$(X_i^{CB}, Y_i^{CB}, Z_i^{CB})$ - real world measured CB centroid \mathbf{i}

Because there are more equations than unknowns the system is over determined, therefore the pseudo inverse of \mathbf{A} is used.

The calibration parameters and the 2-D camera view marker centroids from at least two different camera views are then used to calculate the 3-D real world marker centroids. This is accomplished by re-writing Equations B.6 and Equation B.7 into Equation B.9 and Equation B.10 respectively for camera m , and Equation B.11 and Equation B.12 for camera n .

$$(U_i^m - L_4^m) = (L_1^m - U_i^m L_9^m) X_i^{mn} + (L_2^m - U_i^m L_{10}^m) Y_i^{mn} + (L_3^m - U_i^m L_{11}^m) Z_i^{mn} \quad (\mathbf{B.9})$$

$$(V_i^m - L_8^m) = (L_5^m - V_i^m L_9^m) X_i^{mn} + (L_6^m - V_i^m L_{10}^m) Y_i^{mn} + (L_7^m - V_i^m L_{11}^m) Z_i^{mn} \quad (\mathbf{B.10})$$

$$(U_i^n - L_4^n) = (L_1^n - U_i^n L_9^n) X_i^{mn} + (L_2^n - U_i^n L_{10}^n) Y_i^{mn} + (L_3^n - U_i^n L_{11}^n) Z_i^{mn} \quad (\mathbf{B.11})$$

$$(V_i^n - L_8^n) = (L_5^n - V_i^n L_9^n) X_i^{mn} + (L_6^n - V_i^n L_{10}^n) Y_i^{mn} + (L_7^n - V_i^n L_{11}^n) Z_i^{mn} \quad (\mathbf{B.12})$$

where \mathbf{m} and \mathbf{n} are the camera indices ($\mathbf{m} \neq \mathbf{n}$), \mathbf{i} is the marker number index ($X_i^{mn}, Y_i^{mn}, Z_i^{mn}$) is the \mathbf{i}^{th} calculated real world coordinate marker center calculated from camera \mathbf{m} and \mathbf{n} , (U_i^m, V_i^m) is the \mathbf{i}^{th} marker centers for camera view m , (U_i^n, V_i^n) is the \mathbf{i}^{th} marker centers for camera view n ,

(L_1^m, \dots, L_{11}^m) are the calibration parameters for camera **m**, and (L_1^n, \dots, L_{11}^n) are the calibration parameters for camera **n**.

For the given two cameras, these equations are solved in terms of the 3-D real world marker centroids $(X_i^{mn}, Y_i^{mn}, Z_i^{mn})$. The solution is

$$[X_i^{mn} \ Y_i^{mn} \ Z_i^{mn}]^T = (\mathbf{B}^T \mathbf{B})^{-1} \mathbf{B}^T [U_i^m - L_4^m \ V_i^m - L_8^m \ U_i^n - L_4^n \ V_i^n - L_8^n]^T \quad (\mathbf{B.13})$$

where $(\mathbf{B}^T \mathbf{B})^{-1} \mathbf{B}^T$ is the pseudo inverse and

$$\mathbf{B} = \begin{bmatrix} L_1^m - L_9^m U_i^m & L_5^m - L_9^m V_i^m & L_1^n - L_{9n} U_i^n & L_5^n - L_9^n V_i^n \\ L_2^m - L_{10}^m U_i^m & L_6^m - L_{10}^m V_i^m & L_2^n - L_{10}^n U_i^n & L_6^n - L_{10}^n V_i^n \\ L_3^m - L_{11}^m U_i^m & L_7^m - L_{11}^m V_i^m & L_3^n - L_{11}^n U_i^n & L_7^n - L_{11}^n V_i^n \end{bmatrix}^T.$$